



In Silico Simulations and Functional Cell Studies Evidence Similar Potency and Distinct Binding of Pacific and Caribbean Ciguatoxins

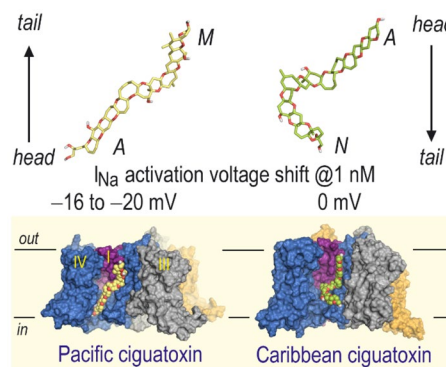
Sandra Raposo-García¹ · David Castro² · Emilio Lence³ · Pablo Estévez² · José Manuel Leão² · Concepción González-Bello³ · Ana Gago-Martínez² · M. Carmen Louzao¹ · Carmen Vale¹ · Luis M. Botana¹

Received: 11 July 2022 / Revised: 21 September 2022 / Accepted: 22 September 2022 / Published online: 8 October 2022
© The Author(s) 2022

Abstract

Ciguatoxins (CTX) cause ciguatera poisoning, which is the most common reported human food poisoning related to natural marine toxins. Pacific ciguatoxins are the most abundant and studied CTX analogues; however, the growing distribution of Caribbean analogues and the limited data available on their biological effects make necessary to re-evaluate their relative potency. For decades, the guidelines established by regulatory agencies have assumed that the potency of the Caribbean CTXs were tenfold lower than the Pacific CTXs. We present here an integrated study involving Neuro-2a cells (the method used worldwide to test ciguatoxins), electrophysiological assays, and in silico simulations that evidence the similar cytotoxicity of Caribbean and Pacific ciguatoxins and their asymmetry binding within sodium channels. The binding mode of the toxins was first explored by molecular docking using the GOLD program and the resulting binary complexes were further studied by Molecular Dynamics simulation studies using the molecular mechanics force field AMBER. The simulation studies explain their distinct impact on the activation potential of the channel as experimentally observed and provide a detailed picture of the effects caused by these toxins on an atomic scale.

Graphical Abstract



Keywords Ciguatoxins · Sodium channels · Molecular modeling · Ciguatera poisoning · Toxicity

✉ Concepción González-Bello
concepcion.gonzalez.bello@usc.es

✉ Ana Gago-Martínez
anagago@uvigo.es

✉ Luis M. Botana
luis.botana@usc.es

Extended author information available on the last page of the article

Abbreviations

CTX	Ciguatoxin
CP	Ciguatera poisoning
EFSA	European food safety authority
FAO	Food and agriculture organization
FDA	Food and drug administration
IC ₅₀	Half-maximal inhibitory concentration
MD	Molecular dynamics
PM	Pore module

TEF	Toxicity equivalency factor
VGSC	Voltage-gated sodium channels
VSM	Voltage-sensing module
WHO	World health organization

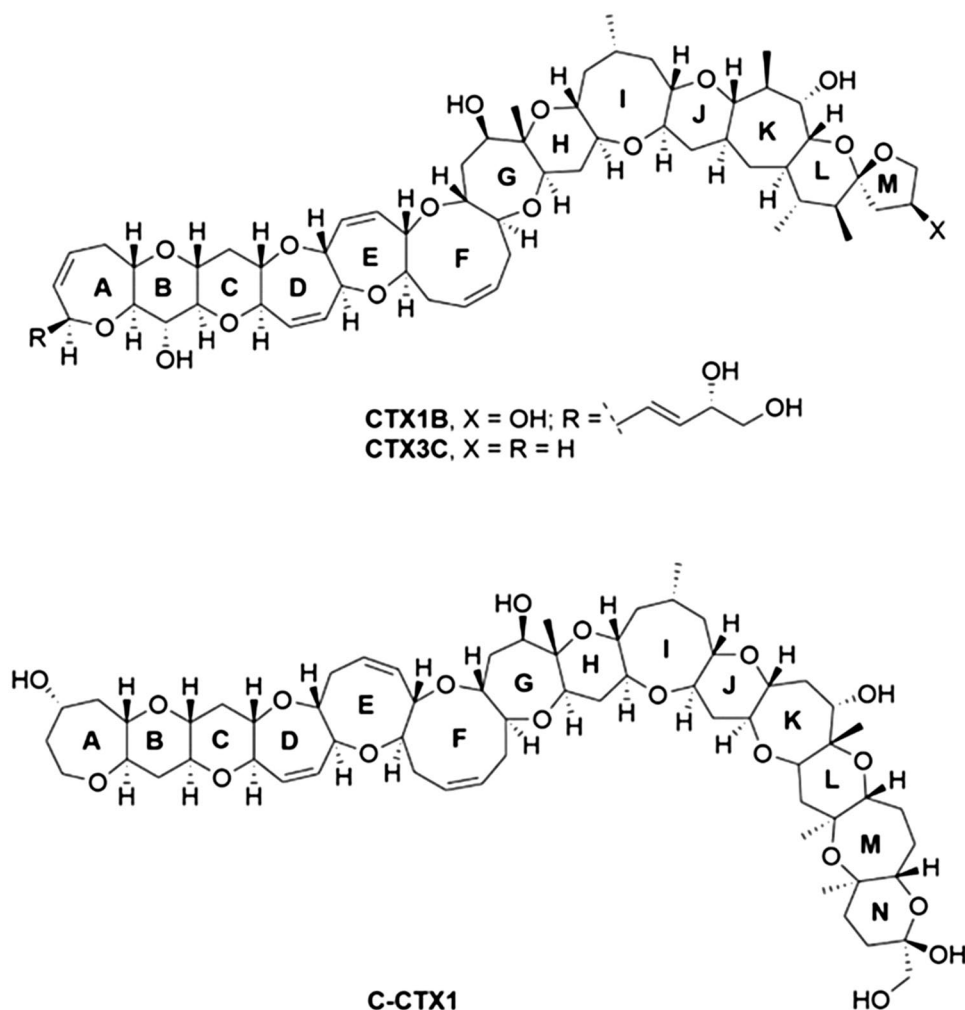
Introduction

Ciguatoxins (CTX) are marine biotoxins produced by benthic dinoflagellates of the genera *Gambierdiscus* and *Fukuyoa* (Gomez et al. 2015; Holmes and Lewis 1994). On the base of their chemical structures, four different ciguatoxin groups were described: Caribbean CTXs (C-CTX1), Indian CTXs (I-CTX1), and Pacific ciguatoxins, which are divided into two different groups, CTX3C and CTX4A and their derivatives as summarized by the FAO/WHO (Food and Agriculture Organization and the World Health Organization) report (FAO 2020). Among these groups, Pacific ciguatoxins analogues (P-CTXs) are the most widely distributed, studied, and evaluated. The chemical structures of Pacific and Caribbean ciguatoxins are represented in Fig. 1.

Regarding C-CTXs, the studies performed until now have shown that the most commonly found analogues are the Caribbean Ciguatoxin-1 and -2, named as C-CTX1 and C-CTX2 (Estevez et al. 2019b). Ciguatoxin-producing dinoflagellates were initially found in Indo-pacific oceans and in the Caribbean Sea reviewed by Shmukler and Nikishin (Shmukler and Nikishin 2017); however, during the last decades, as a possible result of climate change (Ramilo et al. 2021; Xu et al. 2016) and anthropogenic activities, including the globalization of trade, these microalgal organisms have spread to European coasts (Botana 2016; FAO 2020; Otero et al. 2010), and this fact rises the need to fully reevaluate the potency of Caribbean and Pacific ciguatoxin analogues.

CTXs cause in humans the syndrome named ciguatera poisoning (CP) due to the ingestion of high levels of the toxin accumulated by carnivorous fish in their musculature, liver, and viscera after predated herbivorous fish, reviewed by Friedman et al. (2017) (Díaz-Asencio et al. 2019; FAO 2020; Friedman et al. 2017). Nowadays, more than 400 fish species are associated with CP in humans, with barracuda, red snapper, grouper, amberjack, sea bass, surgeonfish, and

Fig. 1 Chemical structure and ring denotation of the principal Pacific and Caribbean ciguatoxins



moray eel as the main responsible of these intoxications (FAO 2020; Pérez-Arellano et al. 2005). Moreover, recently, other species of marine invertebrates such as bivalves, echinoderms, and gastropods were also reported as additional vectors of CP (FAO 2020; Rhodes et al. 2020; Silva et al. 2015). CP is characterized by cold allodynia, gastrointestinal, neurological, and cardiovascular symptoms, starting from 30 min after the ingestion of contaminated fish to 24/48 h and persist for weeks and even months (Friedman et al. 2007). Each year up to 500,000 CP cases might occur globally reviewed by Dickey (2008) (Díaz-Asencio et al. 2019; Dickey 2008; Inserra et al. 2017).

In the last years CP has expanded to new regions such as Canary Islands, Madeira Islands, Selvagens archipelagos, New Zealand, and the Mediterranean Sea (Costa et al. 2018; EFSA 2010; Otero et al. 2010; Tudó et al. 2020). In 2004, CP was first confirmed after consumption of flesh from lesser amberjack (*Seriola rivoliana*) from the Canary Islands, a non-endemic region for CP (Pérez-Arellano et al. 2005) and later on associated with the presence of Caribbean ciguatoxins in Madeira and Canary Islands (Boada et al. 2010; Estevez et al. 2019c, 2020; Otero et al. 2010; Sanchez-Henao et al. 2020). Thus CP is a notifiable disease in the Canary Islands since the year 2015 (Sanchez-Henao et al. 2019) and the current situation in Europe points to an increasing expansion of CTXs (Canals et al. 2021; Diogène et al. 2021); in fact, human intoxications from imported fish have been recently described in Germany (Loeffler et al. 2022). The lack of information regarding the relative toxicity of Pacific and Caribbean ciguatoxins makes it difficult to establish their potency, a remarkable fact since their increasing appearance and distribution raises global public concerns regarding human health.

In vivo studies carried out in the 90s evidenced a half lethal dose (LD_{50}) for intraperitoneal P-CTX of $0.25 \mu\text{g kg}^{-1}$ body weight (Vernoux and Lewis 1997) and $3.6 \mu\text{g kg}^{-1}$ and $1 \mu\text{g kg}^{-1}$, respectively, for C-CTX1 and C-CTX2 (Lewis et al. 1999, 1991). However, the mouse bioassay is currently no longer considered an appropriate method to detect ciguatoxins in fishery products due to poor specificity and ethical concerns (EFSA 2010). In the European Union (EU), seafood products which may contain ciguatoxins are not allowed to be placed on the market (EU 2019). In contrast, the United States Food and Drug Administration (FDA) has established a guidance level for Caribbean CTXs of $0.1 \mu\text{g kg}^{-1}$ C-CTX1 equivalents and $0.01 \mu\text{g kg}^{-1}$ for P-CTX1B (FAO 2020; FDA 2011) based on their intraperitoneal toxicity in mice which implies that Pacific ciguatoxins are tenfold more potent than their Caribbean congeners (Lewis et al. 1991; Vernoux and Lewis 1997).

Nowadays there are several drawbacks which hinder the establishment of the real potency of these emerging marine toxins: (i) the data obtained so far are uncertain because

the presence of CTXs in fish tissues is difficult to detect and quantify (Caillaud et al. 2010), (ii) absence of animal toxicity reports for these compounds, and (iii) CTX doses related with clinical symptoms of CP in humans are not well defined. These factors are aggravated by the lack of certified reference standards for the CTX group of toxins (EFSA 2010). Finally, lethality as reported with the mouse bioassay is not a useful value to quantify CTX potency since these toxins cause complex non-lethal symptoms and CP due to their effect on voltage-gated sodium channels (VGSC) specifically the domain IV of site 5 (FAO 2020). Although the effect of ciguatoxins is primarily on voltage-gated sodium channels (Catterall et al. 1992), these compounds can also alter potassium-gated voltage channels functioning (Hidalgo et al. 2002). The levels of C-CTX allowed in food are $1.8 \mu\text{g kg}^{-1}$ in inedible fish, 0.9 to $< 1.8 \mu\text{g kg}^{-1}$ edible in small quantities, and edible with less than $0.9 \mu\text{g kg}^{-1}$ (Lewis et al. 1999).

The spread worldwide and the scarce reliable information about the biological effects of these emergent toxins in the same cellular model led to several international organizations such as FAO, WHO, and EFSA to highlight the need for a full re-evaluation of the toxicity and relative potencies of these toxins (EFSA 2010; FAO 2020). This work was designed to fully evaluate and compare the cytotoxicity of Pacific and Caribbean ciguatoxin analogues, as well as their effects on the functional activity of sodium channels. Besides, to achieve a better understanding of the experimental results, docking and molecular dynamics (MD) simulations have been used to explore, in atomic detail, the plausible binding mode of these toxins to the α subunit of VGSC, as well as to get an insight of the conformational changes promoted by these compounds. The molecular modeling results on Na_v channels presented here suggest that both analogues bind to sodium channels in an opposite conformation but have similar toxicity as evaluated using internationally adopted methods to detect these toxins (Caillaud et al. 2010; Castro et al. 2020).

Experimental Section

Modeling and Simulation Studies

Building of the Three-Dimensional Model of $\text{Na}_v1.6$ Channel in the Unbound Form

The three-dimensional structure of $\text{Na}_v1.6$ channel was created using the AlphaFold method (Jumper et al. 2021) (UniProt accession code Q9UQD0) and further validated by Molecular Dynamics simulation studies. To this end, the protein was immersed in a cube of $\sim 80,000$ TIP3P water molecules and neutralized by addition of sodium ions (3) using

the molecular mechanics force field ff14SB of AMBER 17 (Case et al. 2017). The residues 1–108, 427–735, and 1778–1980, which correspond to long and unfolded loops not involved in the membrane part of the channel, were deleted for the simulation. Computation of the protonation state of titratable groups at pH 7.0 was carried out using the H⁺⁺ Web server (Gordon et al. 2005). As a result of this analysis, all histidine residues were considered in their neutral forms except H1678. The neutral histidine residues were protonated in ϵ position except H920 and H1354, for which the δ position was selected. Disulfide bridges were used between the following pairs of cysteine residues: C281/C333, C324/C339, C906/C912, C944/C953, C1356/C1376, and C1721/C1736. The minimization of the protein and MD simulation of the resulting minimized structure were carried out following our previously described protocol (Vazquez-Ucha et al. 2021) and 200-ns simulations were performed. The cpptraj module in AMBER 17 was used to analyze the trajectories and to calculate the root-mean-square deviation of atomic positions (*rmsd*) of the protein during the simulation (Roe and Cheatham 2013). The molecular graphics program PyMOL (DeLano 2002) was employed for visualization and depicting protein structures.

Building of the Three-Dimensional Models of Na_v1.6@*ciguatoxin* Binary Complexes

(1) *Ligand preparation*: The geometries of ciguatoxins CTX1B, CTX3C, and C-CTX1 were minimized using a restricted Hartree–Fock (RHF) method and a 6-31G(d) basis set, as implemented in the *ab initio* program Gaussian 09 (Frisch et al. 2009). Partial charges were derived by quantum mechanical calculations using Gaussian 09, as implemented in the R.E.D. Server (version 3.0) (Vanqualef et al. 2011), according to the RESP model (Cornell et al. 1995). The missing bonded and non-bonded parameters were assigned, by analogy or through interpolation, from those already present in the AMBER database (GAFF) (Wang et al. 2006, 2004).

(2) *Docking studies*: The binding mode of ciguatoxins CTX1B, CTX3C, and C-CTX1 were first explored by docking using the program GOLD 2020.2.0 (Jones et al. 1997) and the coordinates of Na_v1.6 channel in the unbound form. The snapshot after 200 ns of simulation was selected. The previously minimized ciguatoxin geometries were used as MOL2 files. Each ligand was docked in 25 independent genetic algorithm (GA) runs, and for each of these, a maximum number of 100,000 GA operations were performed on a single population of 50 individuals. Operator weights for crossover, mutation, and migration in the entry box were used as default parameters (95, 95, and 10, respectively) as well as the hydrogen bonding (4.0 Å) and van der Waals

(2.5 Å) parameters. The position of M388 was used to define the active site, and the radius was set to 30 Å. The GOLD scoring function was used.

MD Simulations Studies of Na_v1.6@*ciguatoxin* Binary Complexes

(1) *Minimization*: Ligand coordinates obtained by docking were employed as starting point for MD simulations of the corresponding binary complexes. The complexes immersed in a cube of TIP3P water molecules and sodium ions were minimized in four stages: (1) initial minimization of the ligands (1000 steps, first half using steepest descent and the rest using conjugate gradient); steps (2), (3), and (4) were performed as steps (a), (b), and (c) in the minimization of the unbound form. A positional restraint force of 50 kcal mol⁻¹ Å⁻² was applied to those unminimized atoms during the first three stages (1–3).

(2) *Simulations*: MD simulations of the Na_v1.6@*ciguatoxin* binary complexes were performed as indicated for the unbound protein form (see above). For Na_v1.6@CTX1B and Na_v1.6@C-CTX1 complexes, simulations of 200 ns were carried out, while for Na_v1.6@CTX3C complex, 100-ns simulation was performed.

Binding Free Energies Calculations

The binding free energy for CTX1B, CTX3C, and C-CTX1 was calculated by the MM/PBSA approach implemented in Amber Tools 17 (Miller et al. 2012) *ante-MMPBSA.py* module was used to create topology files for the complex, enzyme, and ligands and binding free energies were calculated with the *MMPBSA.py* module. A single trajectory approach was used to calculate binding free energies considering only the last 100 ns of the 200-ns MD trajectories. For the 100-ns MD trajectories, the last 80 ns were considered. The Poisson–Boltzmann (PB) and Generalized Born (GB) implicit solvation models were employed. Both models provided similar results.

Toxins and Drugs Used

For the N2a-MTT assay and patch-clamp recordings, C-CTX1-purified solution (25.7 ng/mL) and C-CTX1 Fish Tissue Reference Material (FTRM) (0.284 ± 0.019 ng/g) were purified from an amberjack (*Seriola spp.*) from the Canary Islands (Spain) and were prepared at University of Vigo, in the framework of the project EuroCigua.

For the LC–MS/MS analyses CTX1B, 52-*epi*-54-deoxyCTX1B, 54 deoxyCTX1B, CTX3C, CTX4A, and CTX4B reference materials were kindly provided by Professor Takeshi Yasumoto (Japan Food Research Laboratories, Japan).

C-CTX1 pure standard was kindly provided by Dr. Robert W. Dickey (University of Texas, USA) via Dr. Ronald Manger (Fred Hutchinson Cancer Research Center, Seattle, USA). CTX1B standard solution (4488 ng/mL) was kindly provided by Professor Takeshi Yasumoto (Japan Food Research Laboratories, Japan). CTX3C standard solution (100 ng) was purchased from FUJIFILM Wako Chemicals Europe GmbH (Neuss, Germany).

The stocks standard solutions C-CTX1, CTX1B, and CTX3C used for N2a-MTT assay were diluted in methanol HPLC grade (MeOH, Merck KGaA, Darmstadt, Germany) until a concentration of 10 pg/ μ L and were stored in dry conditions at -20°C .

For electrophysiological recordings Pacific ciguatoxins, CTX3C as well as CTX1B, were purchased from Wako (FUJIFILM Wako Chemicals Europe GmbH, Neuss, Germany) and dissolved in dimethyl sulfoxide (DMSO) at a final concentration of 10 μ M (corresponding to 10,230 ng/mL of CTX3C and 11,113 ng/mL of CTX1B), respectively. For experiments, 1- μ M solutions (1023 ng/mL CTX3C and 1111.3 ng/mL CTX1B) were prepared in Locke's buffer containing (in mM): 154 NaCl, 5.6 KCl, 1.3 CaCl_2 , 1 MgCl_2 , 10 HEPES, and 5.6 glucose, pH 7.4. The maximum solvent concentration used as a control was 0.1% DMSO and had no effect on voltage-gated sodium current amplitude. Similarly, C-CTX1 was dissolved in DMSO at a final concentration of 1 μ M (1141.4 ng/mL C-CTX1) and dilutions were performed in Locke's buffer, from an original solution of 25.7 ng/mL.

Sample Pretreatment

C-CTX1 FTRM was extracted and purified following the conditions described by Estevez et al. (Estevez et al. 2019a). Briefly, Fish tissue (200 g) was extracted twice with acetone (2×600 mL) using an Ultraturrax® homogenizer. Acetone layers were combined (estimated volume of 1200 mL) and evaporated to an aqueous residue using a multievaporator Syncore Polivap set at 45°C . The aqueous residue (estimated volume 150 mL) was extracted twice with diethyl ether (2×200 mL). The combined organic layers (400 mL) were evaporated to a solid residue using a multievaporator Syncore Polivap set at 45°C . The solid residue was dissolved in 90% methanol (60 mL) and defatted with twice the volume of *n*-hexane (120 mL). The methanol residue was evaporated to dryness under reduced pressure and submitted to the purification step.

The purification step was carried out using Solid-Phase Extraction (SPE) cartridges. An equivalent of 15 g of fish tissue was loaded in each SPE cartridge. The solid residue from the extraction was dissolved in ethyl acetate (26 mL) and aliquots of 2 mL were loaded in a Florisil SPE cartridge (J. T. Baker, 500 mg) previously conditioned with ethyl

acetate (3 mL). The cartridge was washed with ethyl acetate (3 mL) and C-CTX1 was eluted with ethyl acetate:methanol 9:1 (v:v) (5 mL). The toxic eluate was evaporated to dryness under a N_2 stream at 40°C . The solid residue was reconstituted in 60% MeOH (26 mL) and aliquots of 2 mL were loaded in a C18 SPE cartridge (SUPELLEAN, Supelco, 500 mg) previously conditioned with 60% MeOH (3 mL). The cartridge was washed with 60% MeOH (3 mL) and C-CTX1 was eluted with 90% MeOH (5 mL). The eluates from C18 SPE were combined and evaporated to dryness being filtered through 0.22- μ m PVDF filter (Syringe Driver filter Unit, Millex®-CV 0.22 μ m, 13 mm).

LC-MS/MS Analysis

LC-MS/MS analyses were performed following the conditions proposed by Estevez et al. (Estevez et al. 2019a) using an Agilent 1290 Infinity LC system coupled to an Agilent 6495 triple quad iFunnel (Agilent Technologies, Waldbronn, Germany).

CTXs were separated using a C18 column (Poroshell 120-EC-C18, 3.0×50 mm, 2.7 μ m, Agilent USA). The column temperature was set at 40°C and the mobile phases for the chromatographic separation were (A) 0.1% formic acid and 5 mM of ammonium formate in water and (B) MeOH. The gradient started at 78% of B with a linear gradient to 88% of B in 10 min, holding 5 min and increasing to 100% of B until 18 min to wash the column. The gradient returned to 78% of B at 18 min and the column was equilibrated during 4 min prior to the next injection. The flow rate was set at 0.4 mL/min and the injection volume was 1 μ L.

The mass spectrometer operated in positive ionization mode (ESI⁺) monitoring by dynamic Multiple Reaction Monitoring (dMRM) the sodium adduct $[\text{M} + \text{Na}]^+$ of the different CTXs as precursor and product ion at a collision energy (CE) of 40 eV. Source and interface parameters were as the following: drying gas flow, 15 L/min, drying gas temperature 290°C , sheath gas flow 12 L/min, sheath gas temperature 400°C , nebulizer pressure 50 psi, fragmentor potential 380 V, nozzle voltage 300 V, and capillary voltage 5000 V.

The following toxins with reference material available were monitored (Table 1): CTX1B, C-CTX1, 52-*epi*-54-deoxyCTX1B, 54-deoxyCTX1B, CTX3C, CTX4A, and CTX4B.

Human Cell Cultures (hNa_v1.6 HEK cells)

Human embryonic kidney cell line (HEK293) stably expressing the human Na_v1.6 alpha subunit of the sodium channels were kindly provided by Dr Andrew Powell (GlaxoSmithKline R&D, Stevenage, UK) cultured in DMEM/F12 medium supplemented with Glutamax, MEM non-essential

Table 1 MRM transitions of the different CTXs monitored by LC–MS/MS

Toxin	Precursor ion [M + Na] ⁺ (<i>m/z</i>)	Product ion [M + Na] ⁺ (<i>m/z</i>)	Fragmentor (V)	CE (eV)	CAV (eV)
CTX1B	1133.6	1133.6	380	40	4
C-CTX1	1163.7	1163.7	380	40	4
52- <i>epi</i> -54-deoxyCTX1B	1117.6	1117.6	380	40	4
54-deoxyCTX1B	1117.6	1117.6	380	40	4
CTX3C	1045.6	1045.6	380	40	4
CTX4A	1083.6	1083.6	380	40	4
CTX4B	1083.6	1083.6	380	40	4

amino acids solution (Gibco, 1% w/v), and 10% fetal bovine serum as previously described (Boente-Juncal et al. 2021). Geneticin (Gibco) was added at a final concentration of 0.4 mg/mL to increase the expression of sodium channels. Cells were seeded at a density of 30,000 cell/mL and maintained at 37 °C in a 5% CO₂/95% O₂ incubator until the cultures reached an 80% of confluence and placed at 30 °C for 24–48 h before electrophysiological measurements (Burbidge et al. 2002).

N2a-MTT Assay

Cytotoxicity assays were carried out using two different batches of Neuro-2a (N2a) cell line (ATCC® CCL-131), purchased from the American Type Culture Collection (LGC standards S.L.U., Barcelona, Spain) and numbered as 63649750 and 70005648. Base culture medium Roswell Park Memorial Institute (RPMI-1640, R8758, Sigma, Irvine, UK) was supplemented with 1% of 100 mM sodium pyruvate (S8636, Sigma, Irvine, UK), 1% of 200 mM L-Glutamine (G7513, Sigma, Irvine, UK), 1% of Penicillin–Streptomycin formed by 5,000 units and 5 mg mL⁻¹, respectively, (P4458, Sigma, St. Louis, MO, USA), and 10% or 5% v/v of fetal bovine serum (FBS, F2442, Sigma, St. Louis, MO, USA) to obtain an adequate complete growth media (RPMI-10 and RPMI-5, respectively). For passing or seeding, cells were unattached with trypsin EDTA solution (1x) (Sigma-Aldrich, St. Louis, MO, USA). Other reagents for N2a-MTT assay include phosphate-buffered saline (PBS), veratridine hydrochloride, ouabain octahydrate, DMSO, and 3-(4,5-dimethylthiazol-2-yl)-2,5-diphenyltetrazolium bromide (MTT), all of them purchased from Sigma-Aldrich (St. Louis, MO, USA).

N2a cells were maintained in T75 flask (Corning, NY, USA) with 30 mL of RPMI-10 at 37 °C in a humidified atmosphere containing 5% CO₂ and subcultured using a split 1:5 regarding initial cell culture every 48 h. The experiments were done for three different cell passages per batch: passages 214/215/224 and 203/205/220 were selected in batch 63649750 and 70005648, respectively.

For the cytotoxicity assay, methanol extracts of CTXs standards (C-CTX1, CTX3C, and CTX1B) were evaluated using the N2a-MTT assay protocol previously described by Castro et al., (2020). Briefly, 40,000 cells were seeded per well into 96-well assay plates (Corning, NY, USA) in 0.2 mL of RPMI-5 and left to grow for 24 h at 37 °C under a humidified atmosphere enriched with 5% CO₂. Then, cells were sensitized with a mixture 10:1 (v/v) of Ouabain/Veratridine solution (O/V). A good sensitivity for detection of CTX-like compounds was reached for a concentration of O/V which provokes a reduction of 20% in cell viability respect to non-sensitized cells.

Ten serial dilutions were prepared from the CTXs stock standard solutions in RPMI-C, and sensitized cells were exposed 16 h to each concentration level, ranging from 0.00019 to 0.019 nM for C-CTX1, 0.0002 to 0.02 nM for CTX1B, and 0.00021 to 0.021 nM for CTX3C, in replicates of four wells. After this time, cell viability was estimated from absorbance due to formazan produced by the colorimetric MTT assay (Mosmann 1983). Absorbance readings were obtained with a multi-well scanning spectrophotometer (Thermo Fisher Scientific, Ratastie, Finland) using 530 nm as testing wavelength and 630 nm as reference wavelength. Absorbance data were expressed as percentage of cell viability relative to control. Resulting values were fitted to a sigmoidal four-parameter logistic function with hill slope (4PL). From these dose–response curves, inhibitory concentrations (IC₅₀), standard concentration required to cause a reduction of 50% in cell viability expressed in nM, were calculated with the SigmaPlot v.12.0 software.

Electrophysiological Recordings

Whole-cell voltage clamp recordings, achieved by gentle mechanical suction of the membrane patch, were performed in the HEK293 cell line expressing the human Na_v1.6 alpha subunit as previously described (Burbidge et al. 2002). Recording electrodes were fabricated from borosilicate glass microcapillaries (outer diameter, 1.5 mm), and the resistance was 5–10 MΩ. The progress of seal formation was evaluated by monitoring the

decrease in membrane resistance. Series resistance was compensated by about 70% with the internal compensation circuitry of the CV-7B current clamp and voltage clamp headstage. Cells were maintained at a holding potential (V_{hold}) of -55 mV and data were recorded after the membrane resistance has stabilized. Voltage-gated sodium currents were recorded using standard whole-cell voltage clamp recordings at room temperature with a Multiclamp 700B amplifier and digitalized with the Digidata 1440A data acquisition system (both from Axon Instruments, California, U.S.A.). Signals were sampled at 50 kHz after low pass Bessel filtering at 10 kHz. Leak currents were subtracted from active currents by the P/N leak protocol provided by the pClamp10 software. After establishing the whole-cell configuration, cells were allowed to stabilize for 5 min before current recording protocols were initiated to ensure adequate equilibration between the internal pipette solution and the cell cytoplasm. Offline analysis was performed with the pClamp10 software (Axon Instruments). Intracellular electrode solution contained (in mM): 120 CsF, 15 NaCl, 10 EGTA, and 10 HEPES (pH 7.25 adjusted with CsOH), while the extracellular solution was Locke's buffer. To obtain the concentration–response data each ciguatoxin was directly added to the recording chamber and in all the experiments the effect of CTXs on VGSC was evaluated 5 min after bath application of each toxin concentration or the corresponding amount of solvent. To record sodium currents (I_{Na}) and the activation of voltage-gated sodium channels voltage steps from -80 to $+80$ mV (10 mV increments, 17 steps and 0.15 s duration) were applied. Data analysis was performed using GraphPad Prism 5. All data are expressed as means \pm SEM of n determinations. Statistical comparisons were performed by one-way analysis of variance (ANOVA) followed by

Dunnett's multiple comparison test. P values < 0.05 were considered statistically significant.

Results

In the present work the binding of Caribbean and Pacific ciguatoxins to sodium channels was studied by an integrated approach that demonstrated similar toxic activity at the cellular level but different interactions with the protein that cause distinct effects on the activation voltage of sodium channels.

Molecular Modeling Studies

The binding mode of CTX1B, CTX3C, and C-CTX1 with the α subunit of the human $\text{Na}_v1.6$ channel was investigated in silico. As no three-dimensional structure of this protein was available, a homology model was constructed using the AlphaFold method (Jumper et al. 2021) and further validated by Molecular Dynamics (MD) simulation studies. To this end, the protein was immersed in a truncated cube of TIP3P water molecules and neutralized by addition of sodium ions using the molecular mechanics force field AMBER 17 (Case et al. 2017). The minimization of the protein and the MD simulation (200 ns) of the resulting three-dimensional structure was carried following our previously reported protocol (Vazquez-Ucha et al. 2021). The reported model in the unbound form is stable as no significant changes were observed during the whole simulation. The latter is easily visualized by the analysis of the root-mean-standard deviation (rmsd) of the whole-protein backbone, which showed relatively low values considering that it is a protein of about 2000 residues (Fig. S1).

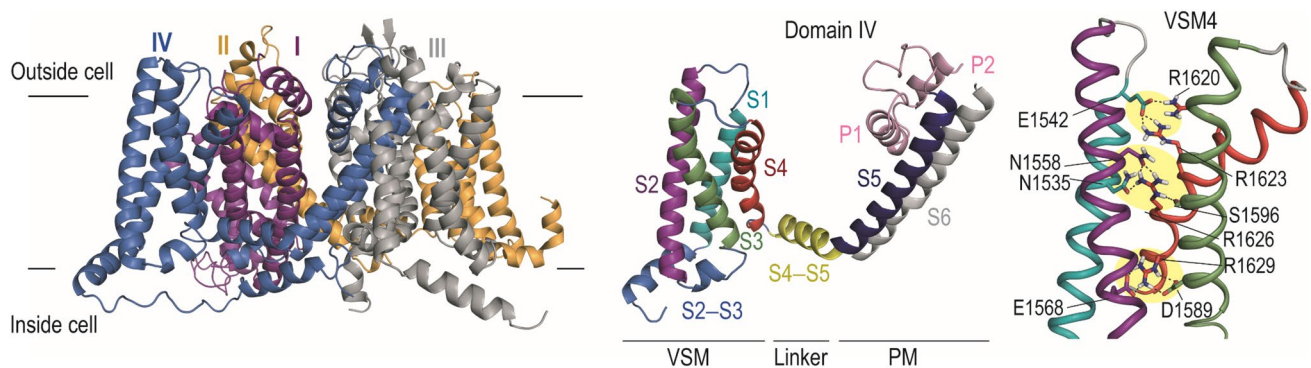


Fig. 2 Overall and detailed views of the three-dimensional model of the α subunit of the human $\text{Na}_v1.6$ channel in the unbound form obtained by MD simulation studies. Snapshot taken after 200 ns of simulation is given. The four domains of the channel (I–IV) are shown in purple, orange, gray, and blue, respectively. Detailed views

of domain IV, as well as the main hydrogen-bonding interactions (black-dashed lines and yellow shadow) of the inner part of the voltage-sensing module 4 (VSM4) are provided. Relevant side-chain residues are shown and labeled

As shown in Fig. 2, the α subunit of the human $\text{Na}_v1.6$ channel consists of four homologous but not identical transmembrane domains (I–IV), each one composed by six transmembrane segments (S1–S6) that form (i) a voltage-sensing module (VSM) containing segments S1–S4; (ii) a pore module (PM) containing segments S5 and S6 and a P-loop that connects them; and (iii) the helical hairpin S4–S5 that connects both modules that seem to act as an elbow in the electromechanical motion of the VSM (Wisedchaisri et al. 2019). Four positive gating charges (arginine residues) that are exquisitely distributed along S4 with their side chains pointing toward segments S1–S3 seem to modulate the VSM function through polar interactions. Thus, these positively charged residues, which are stabilized on the same face of S4 through diverse hydrogen-bonding and electrostatic interactions with the side-chain residues of helices S1–S3, undergo conformational changes as a response to the depolarization and repolarization of the membrane and would trigger long-distance motions in PM to open and close the pore (Ahern et al. 2016; Catterall et al. 2017).

Once the model of the unbound form was validated, the binding modes of Pacific ciguatoxins CTX1B and CTX3C and Caribbean ciguatoxin C-CTX1 were studied by docking using the program GOLD 2020.2.0 (Jones et al. 1997) and the coordinates of $\text{Na}_v1.6$ channel in the unbound form taken after 200 ns of simulation. To define the docking region, it was considered that (i) as brevetoxins, CTXs bind to the S5 segment of domain IV of the channel (Cestele and Catterall 2000; FAO 2020) and (ii) the alanine scanning mutagenesis studies reported by (Konoki et al. 2019) on $\text{Na}_v1.2$ channel showed that changes in the central site of segment S5, specifically residues I1654, G1655, L1656, L1657, and F1659, reduce the affinity of brevetoxin by two–threefold against the wild-type. This region of S5, which is conserved in the $\text{Na}_v1.6$ channel, was therefore selected for binding. To assess the reliability of the GOLD-proposed binding mode, the highest score solutions for each CTX obtained by docking were further analyzed by MD simulation studies following a similar protocol as for the unbound form. Following the same protocol, the binding mode of brevetoxin BTX-3 was also explored for comparison.

The outcomes of these simulation studies showed that all CTXs have in common the following features (Fig. 3): (i) as brevetoxin, these compounds bind to the cleft created by segment S5 of domain IV, segment S6 of domain I, and the P-loop (P1) that connects segments S5 and S6 of domain IV (Fig. S2). The latter binding involves about half of the cyclic polyether skeleton, specifically moieties F–M for CTX1B and CTX3C and moieties A–I for C-CTX1. All CTXs showed to be very stable within the pocket as no significant changes were observed during the whole simulation (Fig. S3), either for the ligand (Fig. S4) or the protein backbone (Fig. S5); (ii) all CTXs interact by hydrogen bonding with

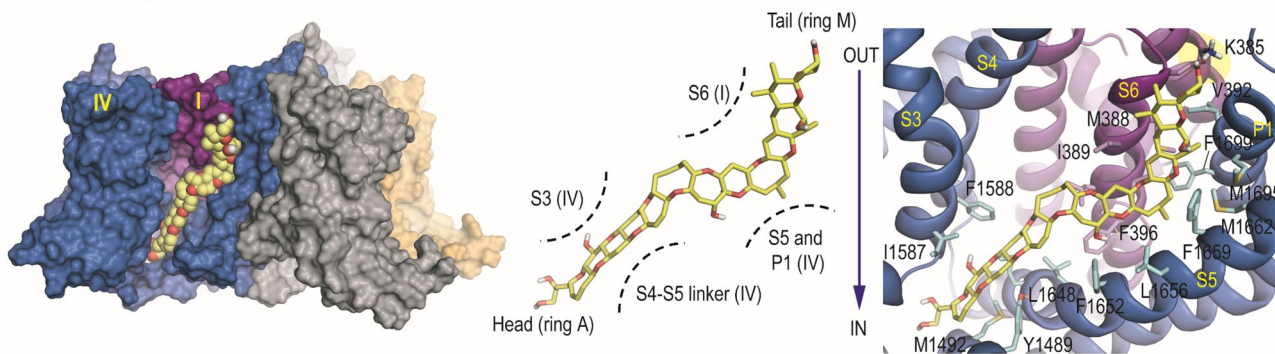
at least one protein residue. CTX1B and C-CTX1 interact with the ϵ -amino group of K385 (S6, domain I) through the hydroxyl group in rings M and A, respectively, while for CTX3C this polar contact occurs between the main carbonyl group in G1584 and the NH group in W1584 and its hydroxyl group (Fig. S6). C-CTX1 establishes additional hydrogen-bonding interactions with residues N1485 and T1482, which are located on the helical hairpin close to segment S5; and (iii) all CTXs lie on the protein cleft thanks to numerous lipophilic interactions, mainly between the axial hydrogen atoms and methyl groups of the linkage between rings and the side-chain residues within the cleft. The latter interactions occur in great extent through both faces of the ciguatoxins polycyclic skeleton. Full details of the residues involved are provided in the supporting information (Table S1).

While no significant differences on the overall binding mode of the two Pacific ciguatoxins were observed, except that CTX3C burrows deeper into the cleft than CTX1B as it lacks substituents on the terminal rings A and M (Fig. 3A, B), the same does not occur for the Caribbean ciguatoxin (Fig. 3C). Thus, the most relevant binding differences among these CTXs are as follows: (i) while Pacific ciguatoxins CTX1B and CTX3C bind to the α subunit of the human $\text{Na}_v1.6$ channel with the ring M pointing toward its extracellular part and ring A toward the cytoplasm [head(IN) to tail(OUT)], C-CTX1 binds in the reverse manner, thus with ring A toward the extracellular part of the channel [tail(IN) to head(OUT)] and (ii) the overall extended conformation of ciguatoxins CTX1B and CTX3C causes binding of moieties A–E of the cyclic polyether skeleton to the interface formed by segment S3 and helical hairpin S4–S5; the curved shape of the Caribbean ciguatoxin C-CTX1 avoids the interaction with the latter site of the channel and facilitates further contacts between its moiety J–N with segment S5 as well as adjacent sites near the cytoplasm.

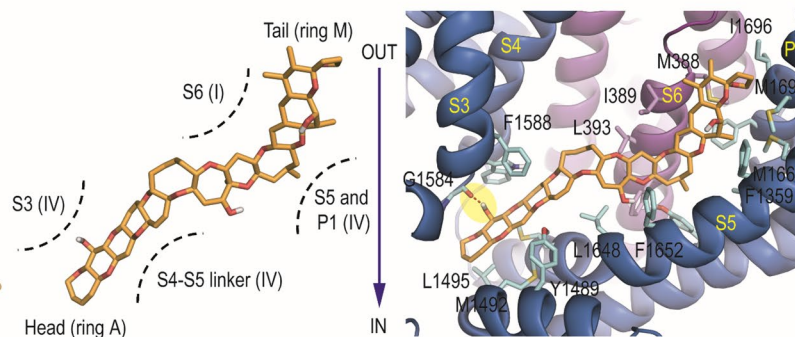
Comparison of the conformation of domain IV of the channel upon CTXs binding with the obtained in the unbound form highlighted relevant differences in the relative arrangement of VSM4 and the helical hairpin S4–S5 in all complexes (Fig. 4). Since the Pacific ciguatoxins CTX1B and CTX3C gave similar results, only the outcomes of ciguatoxins CTX1B and C-CTX1 are presented herein but additional information is given in the supporting information (Fig. S7). For the $\text{Na}_v1.6$ @CTX1B complex, the binding of a fragment of the ciguatoxin skeleton in the interface between segment S3 and linker S4–S5 causes an extended arrangement of the latter relative to segment S5, which implies a loss of the elbow conformation observed in the free form as well as a reduction in the overall plasticity of this region of the protein (Fig. 4A, B).

In addition, the protein site in segment S4 closest to the linker S4–S5 becomes less folded and segments S2 and S3

(A) Nav1.6@CTX1B



(B) Nav1.6@CTX3C



(C) Nav1.6@C-CTX1

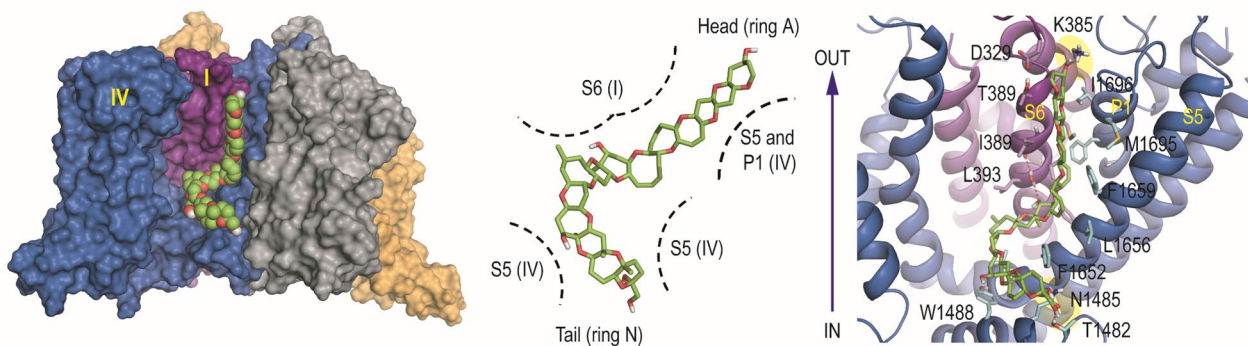


Fig. 3 Overall and detailed views of the three-dimensional models of the α subunit of the human $\text{Na}_v1.6$ channel in complex with CTX1B (A), CTX3C (B), and C-CTX1 (C) obtained by MD simulation studies. Snapshots taken after 200 ns of simulation are given. Domains I–IV are shown in purple, orange, gray, and blue, respectively. In the surface representation, the ciguatoxins are highlighted in spheres. Detailed views of the main contacts between ciguatoxins and the transmembrane segments of the protein are provided. Relevant side-chain residues are shown and labeled. Hydrogen-bonding interac-

tions are provided as dashed lines (red) and with a yellow shadow. Note how both Pacific ciguatoxins bind in a similar manner (head to tail), interacting with the transmembrane segments of domains I and IV: segments S5 (including the P-loops that connect S5 and S6, IV) and S3 (IV), the S4–S5 linker that connect VSM4 with the PM4, and segment S6 (I). On the contrary, C-CTX1 binds with ring A pointing toward the extracellular part of the channel (tail to head) and the interaction with the VSM4 (S3 and S4) is weaker than for Pacific ciguatoxins

move away from the PM4 domain. Helices S3 and S4, and somewhat less pronounced helix S2, twist mainly at their C-terminal part, which is closest to the cytoplasm. As a result of all these conformational changes, the position of

the central gating charge in S4, R1626, is less controlled since the stabilizing partners, the side chains of residues N1558 (S2) and S1596 (S3), move away from its guanidinium group (Fig. 4D, E). Thus, while for the unbound form,

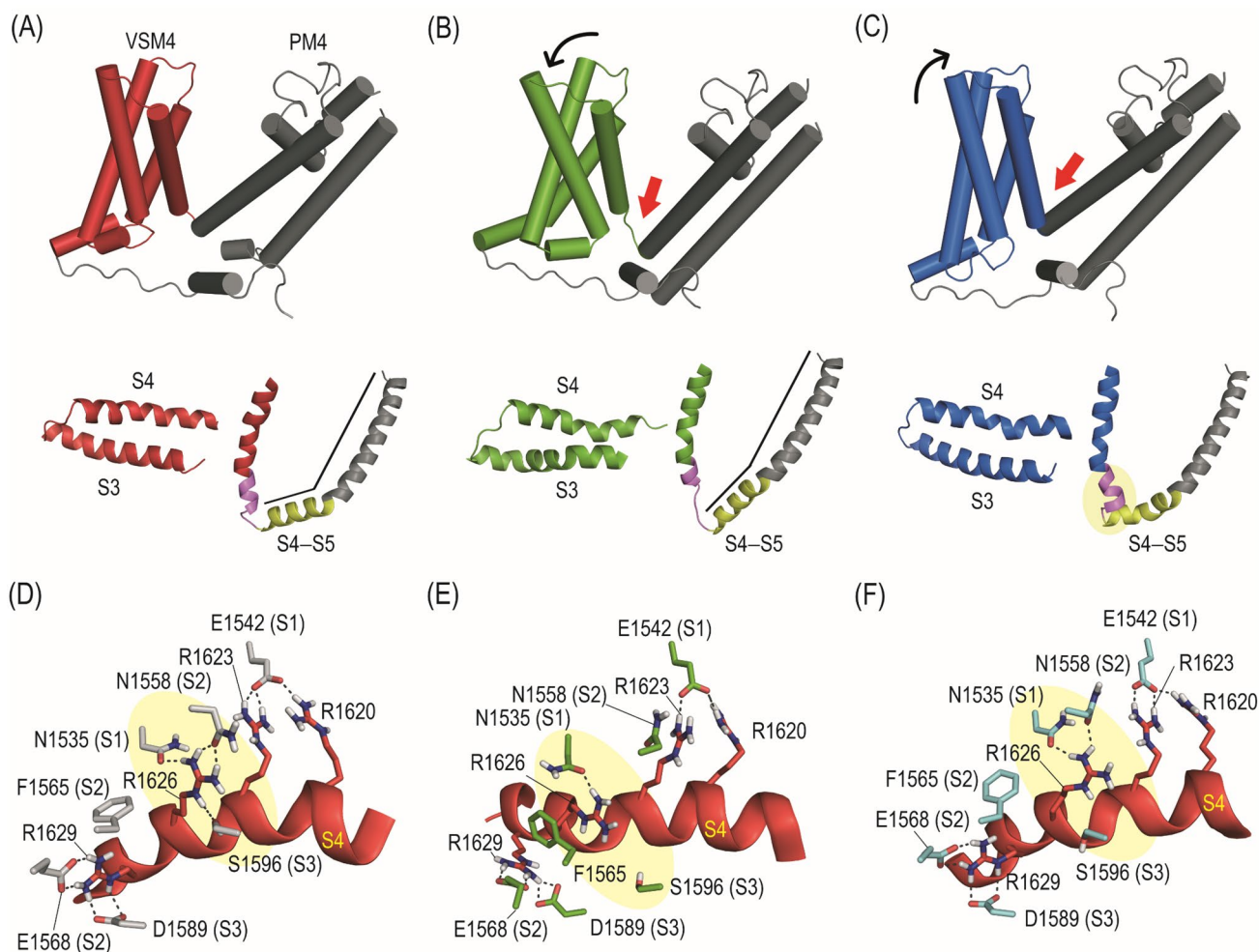


Fig. 4 A–C Comparison of the three-dimensional arrangement of domain IV of the human Na_v1.6 channel in the unbound form (A) and upon ciguatoxins CTX1B (Pacific, B) and C-CTX1 (Caribbean, C) binding. Snapshots taken after 200 ns of simulation and close views of relevant parts of the VSM are given. Note how upon CTX1B binding segment S3 (upper part) is displaced away from PM4 resulting in a new overall arrangement of VSM4, while C-CTX1 binding mainly promotes the folding of the bottom part of segment S4, which is located closer to the linker S4–S5. Note how segments S3 and S4

are twisted in the Na_v1.6@CTX1B complex. D–F Detailed view of the internal polar contacts of the arginine residues located in S4 in the unbound form (D) and the corresponding complexes with CTX1B (E) and C-CTX1 (F). Note how upon binding of CTX1B significant changes in the hydrogen-bonding interactions of residue R1626 (highlighted with a yellow shadow) are observed. In addition, a new arrangement for residue F1565, which is located on top of the guanidinium group of R1626 establishing a strong cation– π interaction, is also identified

the interaction between R1626 and N1558 was observed during ~70% of the simulation with an average distance of 2.9 Å, no contact was observed in the Na_v1.6@CTX1B complex (Fig. S8). A similar trend was identified for residue S1596, which reduces its interaction with R1626 by fourfold in the complex. Remarkably, a significant change is also observed in the disposition of the phenyl group in F1565, which turns to establish a strong cation– π interaction with the guanidinium group of R1626 (Figs. 4E and S9). On the other hand, the impact of C-CTX1 binding on the global arrangement of VSM4 and its relative positioning to PM4 proved to be distinct than the obtained for CTX1B (Fig. 4C, F). For the Na_v1.6@C-CTX1 complex, the results

revealed that (i) a greater folding of the C-terminal part of segment S4, which is shifted toward the linker S4–S5, is observed; (ii) the layered arrangement of the protein region composed by linker S4–S5 and segment S5 is maintained; (iii) no twisting of the helices S2–S4 are observed; (iv) no significant changes in the interactions of residue R1626 as well as motion on the F1565 side chain are identified; and (v) the helical arrangement of linker S2–S3 is lost. As a result of these conformational changes, VSM4 tilts toward segment S5 in its intracellular site.

Despite the differences identified in the binding of the Pacific and Caribbean ciguatoxins with the channel cleft of domain IV, the calculated binding free energies

of these ciguatoxins in the corresponding $\text{Na}_v1.6$ @CTX complex proved to be similar as experimentally observed, with energy values of $-63.5 \pm 0.2 \text{ kcal mol}^{-1}$ and $-61.9 \pm 0.2 \text{ kcal mol}^{-1}$ for CTX1B and C-CTX1, respectively. These calculations were carried out using the MM/PBSA approach in explicit water (generalized Born, GB) and employing frames every 0.1 ns over the last 100 ns of MD simulations as implemented in Amber (Miller et al. 2012).

Functional Consequences of the Different Binding of Pacific and Caribbean ciguatoxins to Human Sodium Channels

C-CTX1 purified solution and C-CTX1 FTRM (Castro et al. 2022) used for the evaluation of the toxicity in functional assays were first analyzed by LC-MS/MS to confirm the presence of C-CTX1 by following the conditions described previously (Estevez et al. 2019a). C-CTX1 was confirmed in the reference material by comparison with authentic C-CTX1. Retention time and ion transition of C-CTX1 selecting the sodium adduct as precursor and product ion m/z 1163.7 $[\text{M}+\text{Na}]^+ / m/z$ 1163.7 $[\text{M}+\text{Na}]^+$ were consistent with the detected in authentic C-CTX1 (Fig. S10).

The quantitation of C-CTX1 was performed with CTX1B applying a correction factor to convert the CTX1B equivalents to C-CTX1 equivalents. CTX1B calibration curve ranged from 0.450 ng mL^{-1} to $44.660 \text{ ng mL}^{-1}$. A C-CTX1 correction factor ($[\text{C-CTX1}] = 0.5 [\text{CTX1B}]$) was obtained by interpolating C-CTX1 pure standard in the CTX1B calibration curve. Therefore, C-CTX1 in the sample was quantified in CTX1B equivalents using the calibration curve. CTX1B eq. were transformed to C-CTX1 eq. with the correction factor previously obtained (Fig. S11). CTX3C and CTX1B, at concentrations between 0.0001 nM and 10 nM shifted the activation voltage of human sodium channels in the negative direction (Fig. 5A). In the absence of toxin the voltage activation of sodium channels occurred approximately at -30 mV . By addition of increasing concentrations of P-CTX analogues (Fig. S11), one-way ANOVA followed by Dunnett's test did not show statistically significant differences between the activation voltage of $\text{Na}_v1.6$ in control conditions and in the presence of 0.0001 nM, 0.001 nM, 0.01 nM, and 0.1 nM neither for CTX1B nor CTX3C (Fig. 5A). The effects on the activation voltage of $\text{Na}_v1.6$ caused by CTX3C and CTX1B were observed at concentrations of 1 nM and higher (Fig. 5A). The sharp negative shift in the activation voltage of sodium channels reached 26 mV after addition of 5 nM CTX1B or 10 nM CTX3C in both cases (Fig. S11). However, for the Caribbean analogue C-CTX1 (Fig. 5A), the activation voltage of sodium channels in control cells was $-33.1 \pm 1.7 \text{ mV}$ ($n = 13$) and $-30.0 \pm 5.7 \text{ mV}$ ($n = 3$) in the presence of 1 nM C-CTX.

Although the effects of the Pacific ciguatoxin analogues on VGSC have been studied previously and these compounds have shown to cause a concentration-dependent decrease in sodium current amplitude (Inserra et al. 2017; Perez et al. 2011; Stevens et al. 2011; Strachan et al. 1999; Yamaoka et al. 2004), the activity of the Caribbean analogues on sodium channels has not been tested so far. In this study the potency of CTX3C and CTX1B on VGSC was re-evaluated and compared, for the first time, with the effect of the Caribbean analogue C-CTX1 in human sodium channels.

Regarding CTX1B in the absence of toxin, the mean peak current was $-1965 \pm 276 \text{ pA}$ ($n = 14$) and it decreased in a concentration-dependent manner in the presence of the different concentrations of CTX1B added to the recording chamber. Thus, peak sodium current was $-1205 \pm 505 \text{ pA}$ after bath application of 0.0001-nM CTX1B ($n = 3$), $-1151 \pm 414 \text{ pA}$ for 0.001 nM ($n = 3$), $-1395 \pm 308 \text{ pA}$ for 0.01 nM ($n = 6$), $-869 \pm 306 \text{ pA}$ for 0.1 nM ($n = 8$), $-375 \pm 144 \text{ pA}$ for 1 nM ($n = 5$), $-393 \pm 199 \text{ pA}$ for 5 nM ($n = 5$), and $-217 \pm 67 \text{ pA}$ for 10 nM ($n = 3$). The normalized peak sodium currents amplitudes in the absence and presence of the different CTX1B concentrations are summarized in Fig. 5B and representative sodium traces in control conditions or in the presence of 1 nM CTX1B are shown in the inset.

In the same context, the response of sodium channels to CTX3C was also evaluated (Fig. 5C). In control cells the peak sodium current was $-1506 \pm 197 \text{ pA}$ ($n = 13$) and it decreased in a concentration-dependent manner in the presence of the different concentrations of CTX3C added to the recording chamber. Thus, peak sodium current was $-1022 \pm 65 \text{ pA}$ after bath application of 0.0001 nM ($n = 5$), $-872 \pm 87 \text{ pA}$ for 0.001 nM ($n = 5$), $-967 \pm 175 \text{ pA}$ for 0.01 nM ($n = 4$), $-933 \pm 212 \text{ pA}$ for 0.1 nM ($n = 7$), $-407 \pm 131 \text{ pA}$ for 1 nM ($n = 3$), $-475 \pm 184 \text{ pA}$ for 5 nM ($n = 3$), and $-525 \pm 210 \text{ pA}$ for 10 nM ($n = 3$). The normalized peak sodium currents in the absence and presence of the different CTX3C concentrations and the representative sodium traces in control conditions or in the presence of 1 nM CTX3C are shown in Fig. 5C.

The evaluation of the effect of C-CTX1 on VGSC was performed at concentrations of 0.0001 nM, 0.001 nM, 0.01 nM, 0.1 nM, and 1 nM, since the matrix effect did not allow the use of higher toxin concentrations because cell seals became unstable. In this case, C-CTX1 caused a decrease of the peak sodium current similar to that caused by the Pacific analogues, and this effect was concentration dependent. In $\text{Na}_v1.6$ human sodium channels, in the absence of toxin the maximum peak sodium current amplitude was $-1916 \pm 306 \text{ pA}$ ($n = 13$). The addition of increasing C-CTX1 concentrations caused a progressive concentration-dependent decrease in the maximum peak sodium current intensity. Thus as shown in Fig. 5D, after bath application of

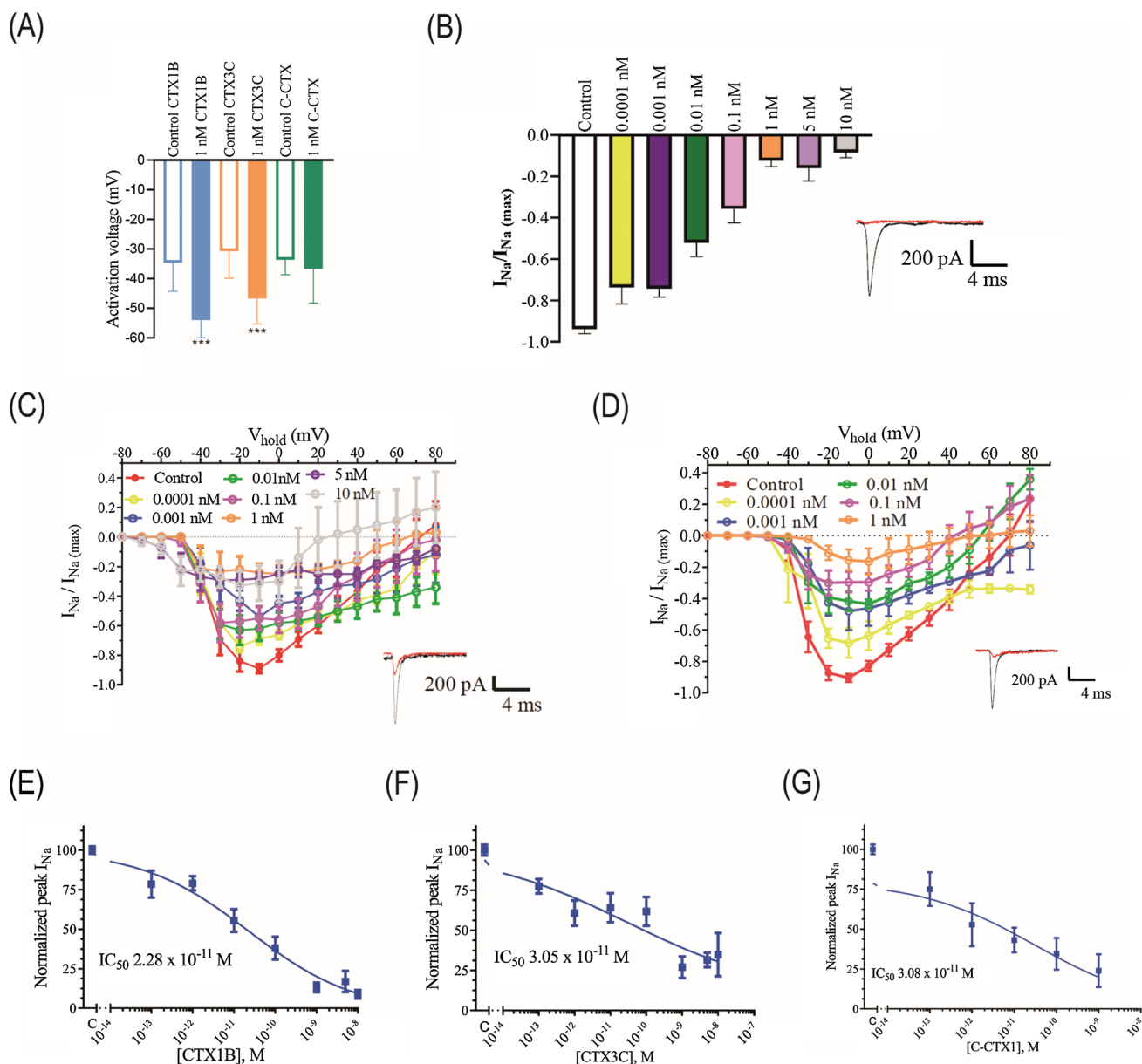


Fig. 5 **A** Effects of Pacific and Caribbean ciguatoxins on the activation voltage of sodium channels. **B–D** Current–voltage relationship for the effect of different concentrations of ciguatoxins CTX1B (**B**), CTX3C (**C**), and C-CTX1 (**D**) on sodium currents and representative sodium currents traces elicited at -20 mV in the absence of toxin

(black) and in the presence of 1 nM of ciguatoxin (red) are shown in the inset. **E–G** Concentration–response graphs indicating the effect of CTX1B (**E**), CTX3C (**F**), and C-CTX1 (**G**) on the normalized peak inward sodium currents at -10 mV and the corresponding IC_{50} obtained in each condition

0.0001-nM C-CTX1 I_{Na} was -1434 ± 89 ($n=3$), -969 ± 71 pA for 0.001 nM ($n=3$), -886 ± 409 pA for 0.01 nM ($n=5$), -705 ± 260 pA for 0.1 nM ($n=5$), and -438 ± 93 pA for 1 nM ($n=3$). Normalized peak sodium currents intensities in the absence and presence of the different C-CTX1 concentrations and representative sodium traces in control conditions and in the presence of 1 nM C-CTX1 are shown in Fig. 5D.

The percent inhibition of the peak inward sodium currents by different concentrations of CTX were used to obtain a concentration–response curve (Fig. 5E–G). Non-linear fit of the data yielded an estimated IC_{50} for CTX1B of 2.28×10^{-11} M (95% confidence interval (CI) from 1.47×10^{-12} M to 3.54×10^{-11} M) (Fig. 5E), while the IC_{50} inhibition of peak inward sodium current for CTX3C was 3.05×10^{-11} M (95% CI from 6.47×10^{-13} to 2.1×10^{-9}) (Fig. 5F) and 3.08×10^{-11} M for the Caribbean analogue

Table 2 Effects of the three ciguatoxin analogues on the activation voltage of VGSC, their IC₅₀, and relative potency taking into account their effect on Na_v1.6 intensity

Analogue	IC ₅₀ I _{Na} inhibition (M)	Relative potency	Na _v activation voltage at 1 nM toxin (mV)	Activation voltage shift (mV)
Control CTX1B			- 34.62 ± 2.7 (n=13)	
CTX1B	2.28 × 10 ⁻¹¹	1.00	- 54.00 ± 4.0 (n=5)	- 20
Control CTX3C			- 30.71 ± 2.4 (n=14)	
CTX3C	3.05 × 10 ⁻¹¹	0.74	- 46.67 ± 2.9 (n=9)	- 16
Control C-CTX1			- 33.64 ± 1.5 (n=11)	
C-CTX1	3.08 × 10 ⁻¹¹	0.74	- 33.33 ± 8.8 (n=3)	0
Control fish extract			- 34.12 ± 1.230 (n=17)	
Fish extract with C-CTX1	1.7 × 10 ⁻¹¹	1.3	- 33.33 ± 3.333 (n=3)	0

C-CTX1 (95% CI from 5.68 × 10⁻¹⁴ to 1.6 × 10⁻⁸ M) (Fig. 5G).

The effects of the three ciguatoxin analogues on sodium channels are summarized in Table 2 and demonstrate that the relative potency of these compounds on sodium channel intensity is similar but they have different effects on voltage channel activation.

Effect of the Samples Extracted from Ciguatera Fish Caught in Canary Island on VGSC

As for the purified toxins, bath application of fish tissue extract (*Seriola spp.*) containing different concentrations of C-CTX1 decreased the peak sodium current in a concentration-dependent manner (Fig. S12). These decreases were slightly lower than the effects observed when cells were exposed to the same concentrations of purified C-CTX1. Figure S12A shows the normalized peak sodium currents in the absence and in the presence of fish extract containing different C-CTX1 concentrations. The percentage inhibition of peak inward sodium currents by different concentrations of fish tissue extract was used to obtain a concentration–response curve (Fig. S12B). Non-linear fit of the data yielded an estimated IC₅₀ inhibition of peak inward sodium current for the fish extract containing C-CTX1 of 1.7 × 10⁻¹¹ M (95% CI from 1.07 × 10⁻¹² to 2.7 × 10⁻¹⁰ M). In this case, as with pure C-CTX1 the shift in the activation voltage was not observed.

N2a-MTT Cytotoxicity Assay

C-CTX1, CTX1B, and CTX3C toxic potency were evaluated under the same conditions in six different days and for two cell batches Dose–response curves were obtained for three analogues and toxic potency was determined from IC₅₀ values (Fig. 6).

For batch 63649750, CTX1B was the most toxic compound, with an IC₅₀ = 1.42 ± 0.14 pM, while C-CTX1 and CTX3C showed approximately the same toxicity, with

values for IC₅₀ of 1.98 ± 0.42 pM and 2.07 ± 0.55 pM, respectively (Table 3). For batch number 70005648, CTX1B yielded an IC₅₀ = 1.14 ± 0.29 pM, while the IC₅₀ values for C-CTX1 and CTX3C were 1.81 ± 0.36 pM and 1.61 ± 0.43, respectively (Table 3). No statistically significant differences were observed between the IC₅₀ of C-CTX1, CTX1B, or CTX3C (Student's *t* test; *p* = 0.612, 0.311, and *p* = 0.217), respectively. Previous studies showed similar toxicity increases, as follows: C-CTX1 ≤ CTX3C < CTX1B (Castro et al. 2020). Toxic potencies of C-CTX1 and CTX3C are estimated using the formula IC₅₀ (CTX1B)/IC₅₀ (C-CTX1 or CTX3C) (Table 3). The three CTXs analogues showed a similar *in vitro* toxicity, and C-CTX1 and CTX3C were only about 0.3-fold less toxic than CTX1B.

Discussion

CP is an emerging food safety hazard. Many studies have been performed aiming to determine the toxicity and the relative potencies for all the CTXs analogues. However, the lack of suitable certified reference materials and the limited amounts of contaminated product available made these tasks a real challenge. So far, most of these studies were performed using P-CTX analogues because they are the most abundant ones; however, CTX group of toxins isolated in the Caribbean and in the Indian Oceans are emerging and spreading worldwide. So far, some agencies as the FDA considered to have different toxic potencies for Pacific and Caribbean CTXs, therefore caution should be taken in using reference materials or tests developed from Pacific ciguatoxin standards (EFSA 2010).

In the decade of the 90s the first comparison between the toxicity of Pacific and Caribbean CTXs was performed using the mouse bioassay (Lewis et al. 1999; Vernoux and Lewis 1997) and the results provided showed a tenfold higher toxicity for Pacific ciguatoxin versus the Caribbean congeners. The mouse intraperitoneal LD₅₀ obtained were 0.25, 2.3, and 0.9 μg kg⁻¹ for P-CTX1, P-CTX 2, and P-CTX

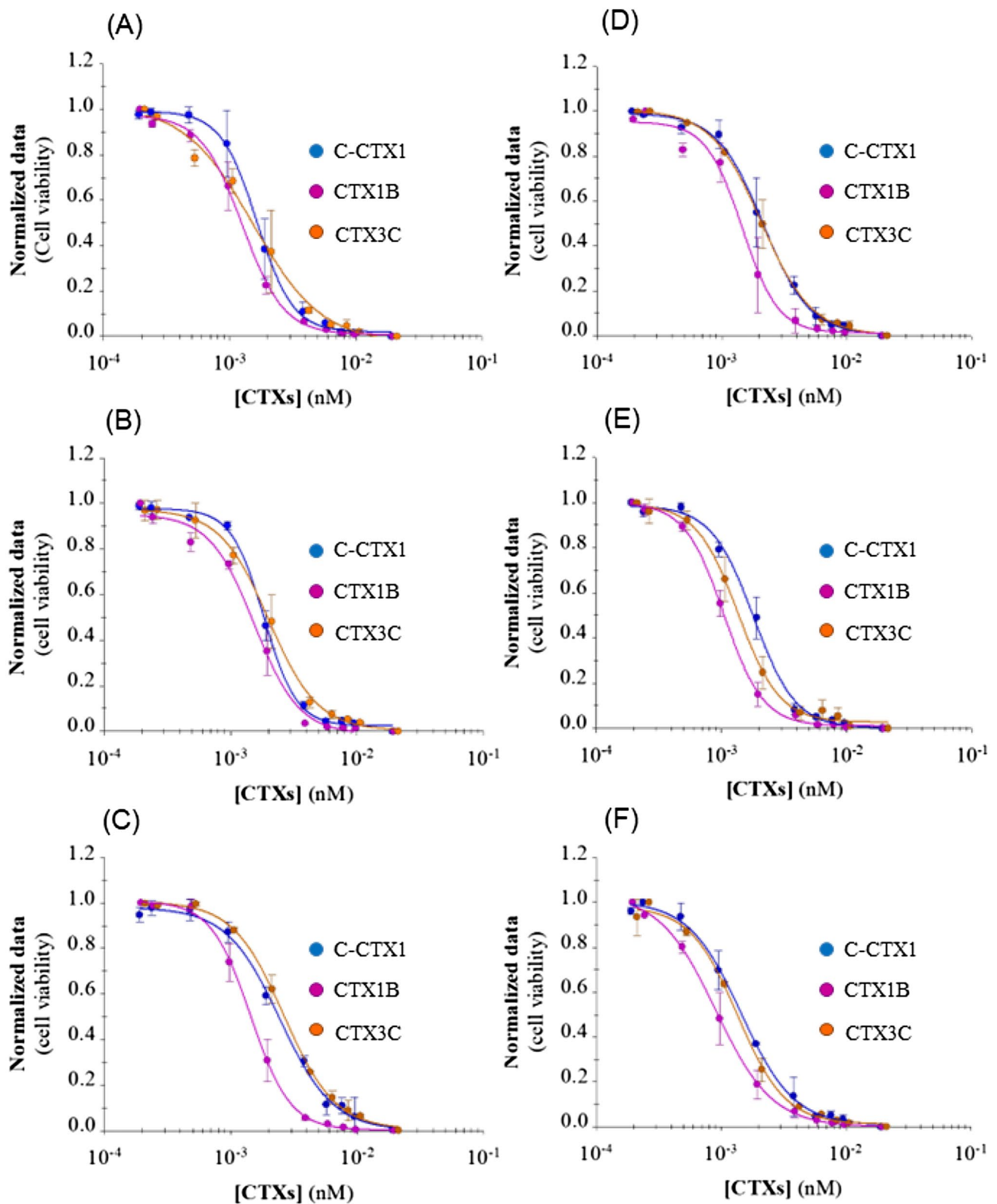


Fig. 6 Dose–response curves of three CTXs standards: C-CTX1, CTX3C, and CTX1B in N2a cells obtained after 16 h exposure to ouabain and veratridine. Left, concentration–response curves from

batch 63649750 at passages number 214 (A), 215 (B), and 224 (C). Right concentration–response curves from batch 70005648 at passages number 203 (D), 205 (E), and 220 (F)

Table 3 Toxic activity (IC_{50} values), slope values, and relative toxic potency (IC_{50} ratio) in different days for the ciguatoxins analogues C-CTX1, CTX1B, and CTX3C

Cell passage (#)	C-CTX1			CTX1B			CTX3C		
	IC_{50} (pM)	Slope	Relative potency	IC_{50} (pM)	Slope	Relative potency	IC_{50} (pM)	Slope	Relative potency
BATCH (#): 63649750									
214	1.65	- 3.1	0.77	1.27	- 2.6	1	1.55	- 1.6	0.82
215	1.84	- 3.4	0.84	1.55	- 2.5	1	2.02	- 2.3	0.76
224	2.45	- 2.1	0.59	1.44	- 2.8	1	2.64	- 2.2	0.54
BATCH (#): 70005648									
203	2.17	- 2.4	0.68	1.47	- 3.0	1	2.10	- 2.2	0.70
205	1.81	- 2.6	0.58	1.05	- 2.8	1	1.36	- 2.6	0.77
220	1.45	- 2.1	0.63	0.92	- 1.9	1	1.36	- 2.3	0.67

3, respectively (Lewis et al. 1991) and 3.6 and 1 $\mu\text{g kg}^{-1}$, for C-CTX1 and C-CTX2 after pH variations. These data were considered by the FDA to establish the current legislation regarding CTX limits in fishery products, assuming that Pacific ciguatoxins and C-CTX1 are the prevalent toxins. These initial studies on the different toxic potencies of Pacific and Caribbean ciguatoxin analogues must be interpreted with caution since the first report on the toxic effect of Caribbean ciguatoxin analogues was performed after the isolation and purification of toxic compounds from thawed flesh fish from the horse-eye jack (*Caranx Lantus*) caught in the French West Indies and autoclaving fish tissues for 30–40 min at 120 °C (Vernoux and Lewis 1997). This procedure was not evaluated to demonstrate that it did not affect the chemical integrity or efficacy of the toxic compounds. It is noteworthy that although, in this paper the authors claimed to follow the same procedure as that followed previously to isolate Pacific ciguatoxins (Lewis and Sellin 1992; Lewis et al. 1991), in the latter case fish viscera was cooked at 70 °C instead of 120 °C. Although ciguatoxins are considered thermostable, their stability is unclear, as there is evidence of interconversion in storage between C-CTX1 and C-CTX2 (Estevez et al. 2019a; Pottier et al. 2001). These valuable initial data were adopted by the expert meeting of FAO to publish their opinion on ciguatera poisoning (FAO 2020) as well as by the FDA to establish the current legislation regarding CTX limits in fishery products (FDA 2011). However, the low availability of purified Caribbean ciguatoxins has prevented further comparison of the toxic potency of the Caribbean and Pacific congeners. Nowadays, several Pacific ciguatoxins with purity higher than 99% are commercially available and were used in this study; however, no available materials for Caribbean ciguatoxins are on the market.

Until now, toxicity equivalency factors (TEFs) and IC_{50} for ciguatoxins analogues were calculated using mainly *in vitro* cytotoxicity assays on neuroblastoma cells. Currently, *in vivo* experiments based on the mouse bioassay are considered of poor specificity besides the experimental ethical

concerns generated by the use of animals (EFSA 2010). The EFSA contaminants panel in the food chain established TEF values for the CTX group of toxins based on their acute intraperitoneal LD_{50} in mice: CTX1 = 1, CTX3C = 0.2, and C-CTX-1 = 0.1. These TEFs should be applied to express individual analogues identified with quantitative detection methods as CTX1B equivalents. But ciguatoxins are a special food safety problem because their toxicity is not associated to lethality but to a chronic syndrome, ciguatera, that may last intermittently several months and shows more than 150 different clinical symptoms (FAO 2020). Therefore, the lethal dose is well above the threshold damage, and lower concentrations should be considered to understand the toxic ciguatera syndrome.

After Lewis and Vernoux *in vivo* research (Lewis et al. 1991; Vernoux and Lewis 1997), other studies were carried out to evaluate the differences in the potency of the different CTXs congeners by the N2a bioassay but in different conditions; thus, the results obtained until date were not clear, varying from a similar toxicity levels for the 3 main analogues (Dechraoui et al. 2007) to a higher toxicity of CTX3C (Loeffler et al. 2021) or even obtaining a higher toxicity of the Caribbean analogue compared to the Pacific one (Dickey 2008).

In the present work we re-evaluated the potency of two Pacific analogues CTX1B and CTX3C as well as the effect of the Caribbean analogue C-CTX1, using N2a bioassay and confirming the results by evaluating the direct effect of the analogues on VGSC. These effects were obtained using the patch-clamp technique, which is the most sensitive assay available so far to study the changes that occur on ion channels. Moreover, these results were confirmed and compared in other laboratories with the cytotoxic results of the same analogues obtained using the most commonly employed *in vitro* technique to evaluate the CTXs cytotoxicity, the Neuro-2a MTT assay, as well as *in silico* evaluation assays. Previous studies have reported the effect of Caribbean ciguatoxin analogues in cultured cells and in VGSC using electrophysiology methods (Hogg et al. 1998, 2002);

Table 4 Comparison of the relative toxicity of CTX1B, CTX3C, and C-CTX1 using *in vitro* techniques with the relative toxicity accepted by authorities

Analogue	I _{Na} inhibition	N2a (B-63649750)		N2a (B-70005648)		EFSA
		Mean	SD	Mean	SD	
CTX1B	1.00	1.00	–	1.00	–	1.00
CTX3C	0.74	0.71	0.14	0.71	0.05	0.2
C-CTX1	0.74	0.73	0.13	0.63	0.05	0.1

however, as far as we know this is the first study analyzing the effect of Caribbean and Pacific ciguatoxins in the same model and using three independent parameters. Besides, in this report the differences in the binding of the CTXs congeners to sodium channels were studied by MD simulation studies, suggesting that the binding of Pacific and Caribbean CTX to sodium channels alter the function of the pore. The results obtained clearly show that the three CTXs analogues caused a similar toxicity, but strikingly CTX3C and C-CTX1 exhibited the same potency, a fact that is at odds with the previously published data (EFSA 2010; Lewis et al. 1991; Vernoux and Lewis 1997). CTX1B had the highest cytotoxic effect and the greatest potency to inhibit sodium currents, followed by CTX3C and C-CTX1 which were very similar on their *in vitro* effects. The higher potency obtained by the fish tissue extract may be due to the matrix effect, since as previously described (Castro et al. 2020) matrix effects can lead to changes in the cytotoxic effect of CTXs depending on the total lipid content of the fish specimens. In this study, the shift in the voltage activation of sodium currents, commonly caused by CTXs, was evaluated and Pacific analogues significantly shifted the voltage activation of sodium channels to more hyperpolarising potentials at concentrations of 1 nM and higher. Again, this observation is in accordance with the previously described effects of ciguatoxins on sodium channels (Inserra et al. 2017; Strachan et al. 1999; Yamaoka et al. 2004). However, this fact could not be corroborated for the Caribbean analogue C-CTX1 nor the fish extract since, in this case, lower concentrations were used (from 0.0001 nM to 1 nM), due to the low availability of compounds. However, at 1 nM, C-CTX1 did not modify the activation potential of sodium channels. The MD simulation studies performed with Pacific ciguatoxins suggested that the shift in the activation voltage of sodium channels caused by these toxins would be due to their interaction with the interface between VSM4 (segment S3) and the linker S4–S5 that connect the latter with segment S5. This binding, which proved to be similar for CTX1B and CTX3C, seems to promote relevant conformational changes in segments S2–S4, altering the ability of the positively charged residues (specifically R1626) to achieve the optimal conformation for establishing polar interactions with the counterion residues inside VSM. As a result of all these changes, the capacity of VSM to perform the required electromechanical motion as a response to the depolarization/repolarization of the membrane would

be modified. These findings would agree with the role of the linker S4–S5 in the established “sliding helix” mechanism of voltage sensing reported by (Wisedchaisri et al. 2019) as the elbow that slide helix S4 through the channel for controlling the motion of the gated residues (arginines) for voltage sensor functions.

On the other hand, the simulation studies carried out with the Na_v1.6@C-CTX1 complex suggested that there is no direct interaction between the Caribbean ciguatoxin and this hinge zone of the channel, as well as no significant changes on the polar interactions network of the positively gated residues. This finding would also justify the experimentally observed lack of shifting on the voltage activation of the channel caused by this toxin. In this case, C-CTX1 seems to reduce the plasticity of the C-terminal part of helix S4, which is connected to the linker S4–S5, which would also compromise the intrinsic sliding of S4 for modulating the channel activity as for the Pacific ciguatoxins. Globally, despite the differences found in the binding mode of both types of ciguatoxins, either in its binding orientation in the channel Na_v1.6 (head to tail and vice versa) or the specific binding pocket of part of its cyclic polyether skeleton, both CTXs seem to freeze the intrinsic motion of the VSM for activity, which would also trigger long-distance conformational changes in PM.

The combined information provided in this work matches, from different approaches and technologies, the current observations regarding the toxicity of CTXs: (i) The calculated binding free energies of -63.5 ± 0.2 kcal mol⁻¹ and -61.9 ± 0.2 kcal mol⁻¹ for CTX1B and C-CTX1 explain the long-term effects of these toxins, as these energies are consistent with high-affinity ligands (high K_{on} and low K_{off}); (ii) the fact that the binding orientation of both types (head to tail and vice versa) generate different modes of voltage sensor activation explains why C-CTX do not modify the activation shift, and this is related to the different observed toxic profiles of P-CTX vs C-CTX. P-CTX is associated to more intense neurological symptoms, while C-CTX is associated to gastrointestinal effects (probably of neurological origin) and later peripheral nervous symptoms (Boucaud-Maitre et al. 2018); and (iii) the activation shift, also observed for other low toxicity molecules, such as gambierol, gambierone, or MTX3 (Raposo-García et al. 2022), contributes to neuronal firing (observed specially in P-CTX toxicity), but

not to mice lethality, that seems to be mainly associated to peak currents, as evidenced by data shown in this paper.

In view of these data, a full re-evaluation of the relative potencies of the CTXs-group of toxins should be pursued using purified compounds and the most sensitive techniques available to guarantee food safety and thus protect human and animal health. Given the TEF results shown in Table 4 that we have obtained by independent studies with patch clamp in human cells and with mouse neuroblastoma, the current legal requirements that assign a tenfold lower potency for Caribbean ciguatoxins do need to be re-evaluated. As shown in Table 4, the mean functional relative potency of the ciguatoxin congeners used in this study was 1 for CTX1B, 0.73 ± 0.036 for CTX3C, and 0.71 ± 0.032 for C-CTX1, summarizing that the potencies of Pacific and Caribbean ciguatoxins are quite similar.

One of the main concerns of this study, which is the same for any other study that uses *Caribbean ciguatoxins*, is the lack of a reference calibrant. Although the quantitation of C-CTX was done against an NMR-quantitated P-CTX, still clearly there is an urgent need of these certified toxins to eliminate quantitative uncertainties.

Conclusion

The results obtained in this study demonstrate that the Pacific analogue CTX1B is the most potent compound of this group, while CTX3C and C-CTX1 caused the same effect confirmed by the cytotoxicity assay and similar effects on the amplitude of sodium currents evaluated by electrophysiological recordings. Both in the cytotoxicity test and in the decrease on sodium current intensity the effect of both analogues CTX3C and C-CTX1 was only 0.3 times lower than that of CTX1B. These data are contrary to what is stated by EFSA and the American FDA, which established a relative potency of C-CTX1 10 times lower than Pacific analogues. Therefore, this study highlights the need to re-evaluate the relative toxicities and potencies of ciguatoxins to establish safety limits for the presence of these emergent toxins in commercialized fish. In addition, docking analyses and simulation studies have demonstrated that the distinct binding mode of ciguatoxins with the channel $\text{Na}_v1.6$ (head to tail and vice versa) justify their different impacts on the activation potential of sodium channels and confirm that this parameter will be more suitable to detect ciguatoxins in suspicious fish samples.

Supplementary Information The online version contains supplementary material available at <https://doi.org/10.1007/s12403-022-00513-0>

Acknowledgements The author's thank Takeshi Yasumoto (Japan Food Research Laboratories) for kindly provided standards of *Pacific*

ciguatoxins. Robert W. Dickey (University of Texas at Austin Marine Science Institute, USA) via Ronald Manger (Fred Hutchinson Cancer Research Center, Seattle, USA) for kindly provided standard of C-CTX1. We are also grateful to the Centro de Supercomputación de Galicia (CESGA) for use of the Finis Terrae computer.

Author Contributions The manuscript was written through contributions of all authors. All authors have given approval to the final version of the manuscript.

Funding Open Access funding provided thanks to the CRUE-CSIC agreement with Springer Nature. The research leading to these results has received funding from the following FEDER-co-funded grants. From Consellería de Cultura, Educación e Ordenación Universitaria, Xunta de Galicia, GRC (ED431C 2021/01, ED431C 2021/29, and the Centro singular de investigación de Galicia accreditation 2019–2022 ED431G 2019/03). From European Union Interreg AlertoxNet EAPA-317-2016, Interreg Agritox EAPA-998-2018, and H2020 778069-EMERTOX, and the EUROCIQUA project: “Risk Characterization of Ciguatera Fish Poisoning in Europe” GP/EFSA/AFSCO/2015/03, co-funded by the European Food Safety Authority (EFSA). From Ministerio de Ciencia e Innovación PID2020-115010RB-I00/AEI/10.13039/501100011033. David Castro (D.C.) financial support for the PhD studies was obtained through EUROCIQUA project: Risk characterization of Ciguatera Fish Poisoning in Europe, framework partnership agreement GP/EFSA/AFSCO/2015/03, co-funded by the EFSA. Pablo Estevez (P.E.) acknowledges financial support from the Xunta de Galicia (Regional Government, Spain) under grant ED481A-2018/207.

Data Availability Enquiries about data availability should be directed to the authors.

Declarations

Conflict of interest The authors declare no financial or commercial conflict of interest.

Open Access This article is licensed under a Creative Commons Attribution 4.0 International License, which permits use, sharing, adaptation, distribution and reproduction in any medium or format, as long as you give appropriate credit to the original author(s) and the source, provide a link to the Creative Commons licence, and indicate if changes were made. The images or other third party material in this article are included in the article's Creative Commons licence, unless indicated otherwise in a credit line to the material. If material is not included in the article's Creative Commons licence and your intended use is not permitted by statutory regulation or exceeds the permitted use, you will need to obtain permission directly from the copyright holder. To view a copy of this licence, visit <http://creativecommons.org/licenses/by/4.0/>.

References


- Ahern CA, Payandeh J, Bosmans F, Chanda B (2016) The hitchhiker's guide to the voltage-gated sodium channel galaxy. *J Gen Physiol* 147(1):1–24. <https://doi.org/10.1085/jgp.201511492>
- Boada LD, Zumbado M, Luzardo OP et al (2010) Ciguatera fish poisoning on the West Africa Coast: an emerging risk in the Canary Islands (Spain). *Toxicol* 56(8):1516–1519
- Boente-Juncal A, Raposo-García S, Louzao MC, Vale C, Botana LM (2021) Targeting chloride ion channels: new insights into the mechanism of action of the marine toxin azaspiracid. *Chem Res*

- Toxicol 34(3):865–879. <https://doi.org/10.1021/acs.chemrestox.0c00494>
- Botana LM (2016) Toxicological perspective on climate change: aquatic toxins. *Chem Res Toxicol* 29(4):619–625. <https://doi.org/10.1021/acs.chemrestox.6b00020>
- Boucaud-Maitre D, Vernoux JP, Pelczar S et al (2018) Incidence and clinical characteristics of ciguatera fish poisoning in Guadeloupe (French West Indies) between 2013 and 2016: a retrospective cases-series. *Sci Rep* 8(1):3095. <https://doi.org/10.1038/s41598-018-21373-2>
- Burbidge SA, Dale TJ, Powell AJ et al (2002) Molecular cloning, distribution and functional analysis of the NAV1. 6. Voltage-gated sodium channel from human brain. *Mol Brain Res* 103(1–2):80–90
- Caillaud A, De la Iglesia P, Darius HT et al (2010) Update on methodologies available for ciguatoxin determination: perspectives to confront the onset of ciguatera fish poisoning in Europe. *Mar Drugs* 8(6):1838–1907
- Canals A, Martínez CV, Diogène J et al (2021) Risk characterisation of ciguatera poisoning in Europe. *EFSA Support Pub* 18(5):6647E
- Case D, Cerutti D, Cheatham T et al (2017) Amber 16 and Amber-Tools17. University of California, San Francisco
- Castro D, Manger R, Vilarino O, Gago-Martinez A (2020) Evaluation of matrix issues in the applicability of the Neuro-2a cell based assay on the detection of CTX in fish samples. *Toxins (basel)*. <https://doi.org/10.3390/toxins12050308>
- Castro D, Estévez P, Leao-Martins JM et al (2022) Preparation of ciguatoxin reference materials from Canary Islands (Spain) and Madeira Archipelago (Portugal) fish. *J Marine Sci Eng* 10(6):835
- Catterall WA, Trainer V, Baden DG (1992) Molecular properties of the sodium channel: a receptor for multiple neurotoxins. *Bull Soc Pathol Exot* 85(5 Pt 2):481–485
- Catterall WA, Wisedchaisri G, Zheng N (2017) The chemical basis for electrical signaling. *Nat Chem Biol* 13(5):455–463. <https://doi.org/10.1038/nchembio.2353>
- Cestele S, Catterall WA (2000) Molecular mechanisms of neurotoxin action on voltage-gated sodium channels. *Biochimie* 82(9–10):883–892
- Cornell WD, Cieplak P, Bayly CI et al (1995) A second generation force field for the simulation of proteins, nucleic acids, and organic molecules. *J Am Chem Soc* 117(19):5179–5197
- Costa PR, Estevez P, Castro D et al (2018) New insights into the occurrence and toxin profile of ciguatoxins in Selvagens Islands (Madeira, Portugal). *Toxins* 10(12):524
- Dechraoui M-YB, Wang Z, Ramsdell JS (2007) Optimization of ciguatoxin extraction method from blood for Pacific ciguatoxin (P-CTX-1). *Toxicol* 49(1):100–105
- DeLano WL (2002) The PyMOL molecular graphics system; DeLano Scientific LLC, Palo Alto, CA. <http://www.pymol.org/>
- Díaz-Asencio L, Clausing RJ, Vandersea M et al (2019) Ciguatoxin occurrence in food-web components of a Cuban coral reef ecosystem: risk-assessment implications. *Toxins* 11(12):722
- Dickey R (2008) Ciguatera toxins: chemistry, biology and detection. In: Botana LM (ed) *Seafood and freshwater toxins*. Taylor and Francis, Boca Raton, FL, pp 479–500
- Diogène J, Rambla M, Campàs M et al (2021) Evaluation of ciguatoxins in seafood and the environment in Europe. *EFSA Support Pub* 18(5):6648E
- EFSA (2010) Scientific Opinion on marine biotoxins in shellfish—emerging toxins: ciguatoxin group. *EFSA J* 8(6):1627
- Estevez P, Castro D, Manuel Leao J, Yasumoto T, Dickey R, Gago-Martinez A (2019a) Implementation of liquid chromatography tandem mass spectrometry for the analysis of ciguatera fish poisoning in contaminated fish samples from Atlantic coasts. *Food Chem* 280:8–14. <https://doi.org/10.1016/j.foodchem.2018.12.038>
- Estevez P, Castro D, Pequeno-Valtierra A, Giraldez J, Gago-Martinez A (2019b) Emerging marine biotoxins in seafood from European Coasts: incidence and analytical challenges. *Foods* 8(5):149. <https://doi.org/10.3390/foods8050149>
- Estevez P, Castro D, Pequeño-Valtierra A et al (2019c) An attempt to characterize the ciguatoxin profile in *Seriola fasciata* causing ciguatera fish poisoning in Macaronesia. *Toxins* 11(4):221
- Estevez P, Sibat M, Leao-Martins JM, Reis Costa P, Gago-Martinez A, Hess P (2020) Liquid chromatography coupled to high-resolution mass spectrometry for the confirmation of Caribbean ciguatoxin-1 as the main toxin responsible for ciguatera poisoning caused by fish from European Atlantic Coasts. *Toxins (basel)* 12(4):267. <https://doi.org/10.3390/toxins12040267>
- EU (2019) Regulation, E. U. No 627/2019. *Off. J. Eur. Union. L* 131/51.
- FAO (2020) Report of the expert meeting on ciguatera poisoning: Rome, 19–23 November 2018, vol 9. <https://apps.who.int/iris/handle/10665/332640>.
- FDA (2011) Guidance for the industry: fish and fishery products hazards and controls guidance. <https://www.fda.gov/regulatory-information/search-fda-guidance-documents/guidance-industry-fish-and-fishery-products-hazards-and-controls>.
- Friedman MA, Arena P, Levin B et al (2007) Neuropsychological study of ciguatera fish poisoning: a longitudinal case-control study. *Arch Clin Neuropsychol* 22(4):545–553. <https://doi.org/10.1016/j.acn.2007.03.003>
- Friedman MA, Fernandez M, Backer LC et al (2017) An updated review of ciguatera fish poisoning: clinical, epidemiological, environmental, and public health management. *Mar Drugs* 15(3):72. <https://doi.org/10.3390/md15030072>
- Frisch M, Trucks G, Schlegel H, et al (2009) Gaussian 09 Revision D. 01, 2009. Gaussian Inc Wallingford CT, 106.
- Gomez F, Qiu D, Lopes RM, Lin S (2015) *Fukuyoa paulensis* gen. et sp. Nov., a new genus for the globular species of the dinoflagellate *Gambierdiscus* (Dinophyceae). *PLoS ONE* 10(4):e0119676. <https://doi.org/10.1371/journal.pone.0119676>
- Gordon JC, Myers JB, Folta T, Shoja V, Heath LS, Onufriev A (2005) H++: a server for estimating pKas and adding missing hydrogens to macromolecules. *Nucleic Acids Res* 33:W368–W371. <https://doi.org/10.1093/nar/gki464>
- Hidalgo J, Liberona JL, Molgo J, Jaimovich E (2002) Pacific ciguatoxin-1b effect over Na⁺ and K⁺ currents, inositol 1,4,5-triphosphate content and intracellular Ca²⁺ signals in cultured rat myotubes. *Br J Pharmacol* 137(7):1055–1062. <https://doi.org/10.1038/sj.bjp.0704980>
- Hogg RC, Lewis RJ, Adams DJ (1998) Ciguatoxin (CTX-1) modulates single tetrodotoxin-sensitive sodium channels in rat parasympathetic neurones. *Neurosci Lett* 252(2):103–106
- Hogg RC, Lewis RJ, Adams DJ (2002) Ciguatoxin-induced oscillations in membrane potential and action potential firing in rat parasympathetic neurons. *Eur J Neurosci* 16(2):242–248. <https://doi.org/10.1046/j.1460-9568.2002.02071.x>
- Holmes MJ, Lewis RJ (1994) Purification and characterisation of large and small maitotoxins from cultured *Gambierdiscus toxicus*. *Nat Toxins* 2(2):64–72. <https://doi.org/10.1002/nt.2620020204>
- Inserra MC, Israel MR, Caldwell A et al (2017) Multiple sodium channel isoforms mediate the pathological effects of Pacific ciguatoxin-1. *Sci Rep* 7:42810. <https://doi.org/10.1038/srep42810>
- Jones G, Willett P, Glen RC, Leach AR, Taylor R (1997) Development and validation of a genetic algorithm for flexible docking. *J Mol Biol* 267(3):727–748. <https://doi.org/10.1006/jmbi.1996.0897>
- Jumper J, Evans R, Pritzel A et al (2021) Highly accurate protein structure prediction with AlphaFold. *Nature* 596(7873):583–589. <https://doi.org/10.1038/s41586-021-03819-2>

- Konoki K, Baden DG, Scheuer T, Catterall WA (2019) Molecular determinants of brevetoxin binding to voltage-gated sodium channels. *Toxins (basel)* 11(9):513. <https://doi.org/10.3390/toxins11090513>
- Lewis RJ, Sellin M (1992) Multiple ciguatoxins in the flesh of fish. *Toxicon* 30(8):915–919. [https://doi.org/10.1016/0041-0101\(92\)90390-q](https://doi.org/10.1016/0041-0101(92)90390-q)
- Lewis RJ, Sellin M, Poli MA, Norton RS, MacLeod JK, Sheil MM (1991) Purification and characterization of ciguatoxins from moray eel (*Lycodontis javanicus*, Muraenidae). *Toxicon* 29(9):1115–1127. [https://doi.org/10.1016/0041-0101\(91\)90209-a](https://doi.org/10.1016/0041-0101(91)90209-a)
- Lewis RJ, Jones A, Vernoux JP (1999) HPLC/tandem electrospray mass spectrometry for the determination of Sub-ppb levels of Pacific and Caribbean ciguatoxins in crude extracts of fish. *Anal Chem* 71(1):247–250. <https://doi.org/10.1021/ac980598h>
- Loeffler CR, Bodi D, Tartaglione L, Dell'Aversano C, Preiss-Weigert A (2021) Improving in vitro ciguatoxin and brevetoxin detection: selecting neuroblastoma (Neuro-2a) cells with lower sensitivity to ouabain and veratridine (OV-LS). *Harmful Algae* 103:101994. <https://doi.org/10.1016/j.hal.2021.101994>
- Loeffler C, Spielmeier A, Friedemann M, Kapp K, Schwank U, Kapfenstein O, Bodi D (2022) Food safety risk in Germany from mislabeled imported fish: ciguatera outbreak trace-back, toxin elucidation, and public health implications. *Front Mar Sci*. <https://doi.org/10.3389/fmars.2022.849857>
- Miller BR 3rd, McGee TD Jr, Swails JM, Homeyer N, Gohlke H, Roitberg AE (2012) MMPBSA.py: an efficient program for end-state free energy calculations. *J Chem Theory Comput* 8(9):3314–3321. <https://doi.org/10.1021/ct300418h>
- Mosmann T (1983) Rapid colorimetric assay for cellular growth and survival: application to proliferation and cytotoxicity assays. *J Immunol Methods* 65(1–2):55–63. [https://doi.org/10.1016/0022-1759\(83\)90303-4](https://doi.org/10.1016/0022-1759(83)90303-4)
- Otero P, Pérez S, Alfonso A et al (2010) First toxin profile of ciguateric fish in Madeira Arquipelago (Europe). *Anal Chem* 82(14):6032–6039. <https://doi.org/10.1021/ac100516q>
- Perez S, Vale C, Alonso E et al (2011) A comparative study of the effect of ciguatoxins on voltage-dependent Na⁺ and K⁺ channels in cerebellar neurons. *Chem Res Toxicol* 24(4):587–596. <https://doi.org/10.1021/tx200043j>
- Pérez-Arellano J-L, Luzardo OP, Brito AP et al (2005) Ciguatera fish poisoning, Canary Islands. *Emerg Infect Dis* 11(12):1981
- Pottier I, Vernoux J-P, Lewis RJ (2001) Ciguatera fish poisoning in the Caribbean islands and Western Atlantic. *Rev Environ Contam Toxicol*. https://doi.org/10.1007/978-1-4613-0143-1_3
- Ramilo I, Figueroa RI, Rayon-Vina F, Cuadrado A, Bravo I (2021) Temperature-dependent growth and sexuality of the ciguatoxin producer dinoflagellate *Gambierdiscus* spp. in cultures established from the Canary Islands. *Harmful Algae* 110:102130. <https://doi.org/10.1016/j.hal.2021.102130>
- Raposo-Garcia S, Louzao MC, Fuwa H, Sasaki M, Vale C, Botana LM (2022) Determination of the toxicity equivalency factors for ciguatoxins using human sodium channels. *Food Chem Toxicol* 160:112812. <https://doi.org/10.1016/j.fct.2022.112812>
- Rhodes LL, Smith KF, Murray JS, Nishimura T, Finch SC (2020) Ciguatera fish poisoning: the risk from an Aotearoa/New Zealand perspective. *Toxins (basel)*. <https://doi.org/10.3390/toxins12010050>
- Roe DR, Cheatham TE 3rd (2013) PTRAJ and CPPTRAJ: software for processing and analysis of molecular dynamics trajectory data. *J Chem Theory Comput* 9(7):3084–3095. <https://doi.org/10.1021/ct400341p>
- Sanchez-Henao JA, Garcia-Alvarez N, Fernandez A et al (2019) Predictive score and probability of CTX-like toxicity in fish samples from the official control of ciguatera in the Canary Islands. *Sci Total Environ* 673:576–584. <https://doi.org/10.1016/j.scitotenv.2019.03.445>
- Sanchez-Henao A, García-Álvarez N, Sergent FS et al (2020) Presence of CTXs in moray eels and dusky groupers in the marine environment of the Canary Islands. *Aquat Toxicol* 221:105427. <https://doi.org/10.1016/j.aquatox.2020.105427>
- Shmukler YB, Nikishin DA (2017) Ladder-shaped ion channel ligands: current state of knowledge. *Mar Drugs* 15(7):232. <https://doi.org/10.3390/md15070232>
- Silva M, Rodriguez I, Barreiro A et al (2015) First report of ciguatoxins in two starfish species: *Ophidiaster ophidianus* and *Marthasterias glacialis*. *Toxins (basel)* 7(9):3740–3757. <https://doi.org/10.3390/toxins7093740>
- Stevens M, Peigneur S, Tytgat J (2011) Neurotoxins and their binding areas on voltage-gated sodium channels. *Front Pharmacol* 2:71. <https://doi.org/10.3389/fphar.2011.00071>
- Strachan LC, Lewis RJ, Nicholson GM (1999) Differential actions of pacific ciguatoxin-1 on sodium channel subtypes in mammalian sensory neurons. *J Pharmacol Exp Ther* 288(1):379–388
- Tudó Á, Toldrà A, Rey M et al (2020) Gambierdiscus and Fukuyoa as potential indicators of ciguatera risk in the Balearic Islands. *Harmful Algae* 99:101913. <https://doi.org/10.1016/j.hal.2020.101913>
- Vanquelef E, Simon S, Marquant G et al (2011) R.E.D. Server: a web service for deriving RESP and ESP charges and building force field libraries for new molecules and molecular fragments. *Nucleic Acids Res* 39:W511–W517. <https://doi.org/10.1093/nar/gkr288>
- Vazquez-Ucha JC, Rodriguez D, Lasarte-Monterrubio C et al (2021) 6-Halopyridylmethylidene penicillin-based sulfones efficiently inactivate the natural resistance of *Pseudomonas aeruginosa* to beta-Lactam antibiotics. *J Med Chem* 64(9):6310–6328. <https://doi.org/10.1021/acs.jmedchem.1c00369>
- Vernoux J-P, Lewis RJ (1997) Isolation and characterisation of Caribbean ciguatoxins from the horse-eye jack (*Caranx latus*). *Toxicon* 35(6):889–900. [https://doi.org/10.1016/s0041-0101\(96\)00191-2](https://doi.org/10.1016/s0041-0101(96)00191-2)
- Wang J, Wolf RM, Caldwell JW, Kollman PA, Case DA (2004) Development and testing of a general amber force field. *J Comput Chem* 25(9):1157–1174. <https://doi.org/10.1002/jcc.20035>
- Wang J, Wang W, Kollman PA, Case DA (2006) Automatic atom type and bond type perception in molecular mechanical calculations. *J Mol Graph Model* 25(2):247–260. <https://doi.org/10.1016/j.jmgm.2005.12.005>
- Wischedchaisri G, Tonggu L, McCord E et al (2019) Resting-state structure and gating mechanism of a voltage-gated sodium channel. *Cell*. <https://doi.org/10.1016/j.cell.2019.06.031>
- Xu Y, Richlen ML, Liefer JD et al (2016) Influence of Environmental variables on *Gambierdiscus* spp. (Dinophyceae) growth and distribution. *PLoS ONE* 11(4):e0153197. <https://doi.org/10.1371/journal.pone.0153197>
- Yamaoka K, Inoue M, Miyahara H, Miyazaki K, Hiram M (2004) A quantitative and comparative study of the effects of a synthetic ciguatoxin CTX3C on the kinetic properties of voltage-dependent sodium channels. *Br J Pharmacol* 142(5):879–889. <https://doi.org/10.1038/sj.bjp.0705852>

Publisher's Note Springer Nature remains neutral with regard to jurisdictional claims in published maps and institutional affiliations.

Authors and Affiliations

Sandra Raposo-García¹  · David Castro² · Emilio Lence³ · Pablo Estévez² · José Manuel Leão² · Concepción González-Bello³ · Ana Gago-Martínez² · M. Carmen Louzao¹ · Carmen Vale¹ · Luis M. Botana¹

Sandra Raposo-García
sandra.raposo.garcia@usc.es

David Castro
dcastro@uvigo.es

Emilio Lence
emiliojose.lence@usc.es

Pablo Estévez
paestevez@uvigo.es

José Manuel Leão
leao@uvigo.es

M. Carmen Louzao
mcarmen.louzao@usc.es

Carmen Vale
mdelcarmen.vale@usc.es

¹ Departamento de Farmacología, Farmacia y Tecnología Farmacéutica, Facultad de Veterinaria, Universidade de Santiago de Compostela, Campus Universitario s/n, 27002 Lugo, Spain

² Biomedical Research Center (CINBIO), Department of Analytical and Food Chemistry, University of Vigo, Campus Universitario de Vigo, 36310 Vigo, Spain

³ Centro Singular de Investigación en Química Biolóxica E Materiais Moleculares (CiQUS), Departamento de Química Orgánica, Universidade de Santiago de Compostela, Jenaro de la Fuente s/n, 15782 Santiago de Compostela, Spain